

Contract No. NAS-1-5743

NASA CR-66322

ELECTROFORMING ALUMINUM COMPOSITES

FOR

SOLAR ENERGY CONCENTRATORS

FINAL REPORT

Prepared for

LANGLEY RESEARCH CENTER  
NATIONAL AERONAUTICS & SPACE ADMINISTRATION  
LANGLEY STATION  
HAMPTON, VIRGINIA

19 May 1967

GPO PRICE \$ \_\_\_\_\_

CFSTI PRICE(S) \$ \_\_\_\_\_

Hard copy (HC) 2.00

Microfiche (MF) 2.00

ff 653 July 65

FACILITY FORM 602	<b>N67-26636</b>	
	(ACCESSION NUMBER)	(THRU)
	<b>73</b>	<b>1</b>
	(PAGES)	(CODE)
	<b>N-66322</b>	<b>15</b>
	(NASA CR OR TMX OR AD NUMBER)	(CATEGORY)

GENERAL ELECTRIC

Re-Entry Systems Department

ELECTROFORMING ALUMINUM COMPOSITES FOR SOLAR ENERGY CONCENTRATORS

By A. G. Buschow, I. J. Hess, and F. J. Schmidt

Distribution of this report is provided in the interest of information exchange. Responsibility for the contents resides in the authors or organization that prepared it.

Prepared under Contract No. NAS 1-5743 by  
GENERAL ELECTRIC COMPANY  
RE-ENTRY SYSTEMS DEPARTMENT  
Philadelphia, Pennsylvania

for

NATIONAL AERONAUTICS AND SPACE ADMINISTRATION

## T A B L E   O F   C O N T E N T S

ABSTRACT..	v
SUMMARY..	1
INTRODUCTION.....	3
ELECTROFORMING PROCESS STUDIES	4
EQUIPMENT STUDY.	13
CONCENTRATOR FABRICATION	15
CONCLUSIONS.	20
TABLES	21
FIGURES.	25
APPENDIX A - PHYSICAL PROPERTY MEASUREMENTS.	47
APPENDIX B - ALUMINUM ELECTROFORMING PROCEDURE IN PILOT CELL	48
APPENDIX C - OPTICAL INSPECTION OF MIRROR.	51
TABLES AND FIGURES	53
REFERENCES	69



## ABSTRACT

This report describes the tests, experiments, developments and studies relating to the optimization of the aluminum electro-deposition process which was developed on a prior contract, NAS 1-3309. Included are the efforts towards increasing the strength of the aluminum deposits by codeposition of glass fibers and hollow silica microspheres, as well as a preliminary design of a plating cell, scaled up by a factor of 15, which would be suitable for electroforming up to 10 feet diameter solar concentrators.

Significant increases in electroform strength were achieved. The ultimate tensile strength and yield point @0.2% offset were increased by 87% and 115%, respectively, for glass fiber-aluminum composites vs plain electroformed aluminum. The laboratory reinforcing process was successfully transplanted into the 200 gallon pilot cell.

The pilot cell built under the previous NAS 1-3309 contract was modified to improve operation and to evaluate potential scale up procedures and designs. A number of 30-inch solar concentrators were electroformed in the modified pilot cell. These included glass fiber and silica microsphere codeposition runs.

## ELECTROFORMING ALUMINUM COMPOSITES FOR SOLAR ENERGY CONCENTRATORS

by A. G. Buschow, I. J. Hess, and F. J. Schmidt  
General Electric Company  
Re-Entry Systems Department

### SUMMARY

The aluminum electroforming process was significantly advanced under the NAS 1-5743 contract, described herein.

The four broad areas of significant activities were:

- a) Laboratory cell studies, aimed at further improving the aluminum electroforming process developed under the prior contract, NAS 1-3309.
- b) Modification of the pilot cell to incorporate any improvements.
- c) Operation of the pilot cell, as shown by the production of four 30-inch diameter solar concentrators.
- d) Design of a plating cell scaled up 15 fold (3000 gallons).

The program achieved success in most, but not all, areas. The laboratory studies were eminently successful, not only in refining the basic process, but also by achieving significant strengthening of the deposit. Glass fibers and hollow silica microspheres were successfully, and reproducibly, codeposited with the aluminum, to give reinforced composites. The significance of this technique can hardly be overemphasized. This is a room temperature process and, thus, does not deteriorate the fibers, is well applicable to other, high strength fibers, and is also applicable to produce composites of any geometry. This fills a valid need in present technology.

By glass fiber incorporation of aluminum electroforms, the U.T.S. was increased by a factor of 1.87 and the yield point by a factor of 2.15. This appears the most promising area for further development work, not only because of the practical significance of the process but because theoretically further dramatic increases are possible.

Other significant improvements were the elimination of pinholes in the deposit. Previously, even 10 mil thick deposits showed visible pinholes, the present deposits were gastight at a mere 3 mil thickness.

The pilot cell was modified and it operated very satisfactorily throughout the program. The major modifications were:

- a) Improved cooling and condensing system, which just about eliminated the previously enormous ether losses.
- b) Direct drive cathode rotation, which in conjunction with the redesigned recirculation path, reduced the deposit roughness. The outlet orifice of the recirculation system was modified several times during the present runs, but further runs are needed for optimization.

- c) Tank cover modifications now permit a rapid, controllable activation and entrance of the substrate into the cell. This used to be a major problem in the previous cell.
- d) Polytetrafluoroethylene tanklining, which was highly successful in the previous cell, failed rapidly this time, due to the insurer's requirement of electrically grounding the tank. Due to bipolar behavior of the tank, the lining was lifted off. Solution contamination and undefinable current distribution were the consequences.
- e) The filters, left unchanged from the previous contract, were very much undersized for the new, improved pump - circulation, piping, and cell design - and represented by far the least satisfactory equipment. These filters were originally designed for alternating vacuum-pressure circulation, and their effective area should be increased now by a factor of at least 10.

Operation of the pilot cell was highly satisfactory excepting the undersized filter and the tanklining, as noted above. Still, the production of the four deliverable concentrators presented unforeseen problems.

The original schedule called for the pilot cell to go on stream early in August, 1966. Due to unforeseen problems plaguing two subcontractors, as well as safety related modifications required by our insurer, the start-up date was four months late, leaving practically no time for experimental runs in the pilot cell.

The glass master developed several cracks, and consequently distortions in its first use. These were caused by residual stresses from the fabrication, and were unrelated to our process. The cracks did not propagate, and no new cracks appeared during five additional runs.

In the first run with the glass master, laminations occurred within the aluminum deposit and at the aluminum-silver interface. While the geometry and the surface of the unaffected areas (approx 75% of the surface) were very good, the mirror was cut up for investigation. It was found, that gas bubbles entering the bath during purging of the filter, after replacing the clogged filter bed, were responsible for periodic passivation of the aluminum surface. Lamination of the aluminum deposit did not occur in the subsequent runs, after modification of the filter purge technique.

The adhesion between the silvered glass and the aluminum deposit was brought under control only in the last two runs, although the areas affected diminished in each run, due to continuous modifications and improvements in the pretreatment cycles.

The last two runs finally solved the adhesion problem by two different approaches: In one, excellent adhesion was achieved, in the other, the glass was coated with a very thin silver parting layer, treated for non-adhesion and this was removed from the mirror at the completion of the process.

The first run, which was an equipment "shake-down" run, employed a 12" nickel master and therefore did not need a conducting silver layer, had no lamination problem and produced an excellent mirror. Because of its small size, it was not in the path of the gas bubbles from the filter return.

In the NAS 1-3309 program the covering knife-edge could not be bridged across with aluminum. This problem was now successfully solved and excellent bridging was obtained.

A preliminary design, scaling up the equipment and process 15-fold was prepared. This incorporates the best up-to-date knowhow.

## INTRODUCTION

The previous contract, NAS 1-3309 (See Ref. 1) succeeded in making large-scale aluminum electroforming - which eluded so many investigators - a practical reality. Although the basic soundness of the process was clearly demonstrated and aluminum electroforming technology was considerably advanced, the process still had some shortcomings and required additional investigation. Also, the General Electric Company had previously demonstrated the feasibility of incorporating glass fibers and other materials into the electroformed aluminum deposit. The potential application for these high-strength composites recommended scale-up of the process parameters.

The present contract, NAS 1-5743 was conceived to advance further the state of the art and has set forth four specific objectives:

- a) Improve the quality of aluminum electroforms.
- b) Strengthen the electroformed aluminum deposits.
- c) Determine the feasibility of electroforming aluminum solar concentrators as large as 10' in diameter.
- d) Improve the quality of electroformed aluminum solar concentrator models.

The first half of the investigation was conducted in the laboratory cell and later efforts were directed to incorporating all new developments into the pilot cell, originally fabricated under NASA Contract NAS 1-3309. Additional scale-up data were then to be secured from pilot cell electroforming runs.

These objectives were largely met. However, the time available for experimentation in the scaled-up facility fell far short of the planned schedule because of nonrecurrent problems associated with obtaining equipment, components and permits. The stated tasks were completed but could not be optimized in every case.

Despite, this singular difficulty, the work produced some spectacular results. Highly promising fiber reinforced aluminum composites were fabricated by electroforming. Pure aluminum deposit test samples showed superior characteristics as pressure vessel liners. There was a renewed interest in cladding applications.



It was demonstrated that the process is very controllable and safe. Large scale equipment was refined to a degree where aluminum electroforming would soon become just one of the routine electroforming processes.

## ELECTROFORMING PROCESS STUDIES

The experimental program, described below, was conducted primarily in the laboratory cell. Various pertinent facets of the electroforming process were investigated to better define a number of process parameters.

### Plating Bath Study

Study areas were as follows:

Bath Temperature Control - A lower electrical resistance in the ethereal bath is desirable because in the past much heat was generated in the electroforming operation. Enormous quantities of ether and aluminum chloride were lost through evaporation (up to 20% of initial volume), therefore the bath composition could not be held constant, the condensing system kept clogging up and premature separation of the deposit from the master occurred due to temperature fluctuation. The first approach evaluated was the modification of the plating bath composition for lowering the ohmic resistance.

A number of 3.4M  $\text{AlCl}_3$  - ether solutions were prepared containing varying  $\text{LiAlH}_4$  content (none, 0.4M, 0.6M, 0.8M, 1.0M, 1.2M and 1.4M, respectively). The electrical characteristics for the freshly prepared solutions were measured at 1-inch, 2-inch and 3-inch electrode spacings. These data are tabulated and presented graphically in Figures 1 through 7. The polarization potential of approximately 0.6 volts, previously reported for the 3.4M  $\text{AlCl}_3$  - 0.4M  $\text{LiAlH}_4$  - ether bath, was observed to extend up through 0.6  $\text{LiAlH}_4$  concentration and significantly decrease at high hydride concentration.

The variation of the specific resistance of a 3.4M  $\text{AlCl}_3$  - ether solution with  $\text{LiAlH}_4$  content appears in Figure 8. Minimum resistance occurs at 1.2M  $\text{LiAlH}_4$  (about a 1:3 molar ratio of  $\text{LiAlH}_4$  to  $\text{AlCl}_3$ ). However, the decreased solution resistance is offset by many negative factors - an observed bath instability (formation of insoluble residues): reduced cathode efficiency; higher stress levels in the electroform, particularly for a freshly prepared bath; and a more difficultly filterable solution.

Increased  $\text{AlCl}_3$  content did not appreciably reduce solution electrical resistance. Also, the solubility limit was soon reached after a 3.4M  $\text{AlCl}_3$  concentration. Significant additions could not be made. On the other hand, while the IR heating was not reduced to an appreciable degree, the ether vaporization losses were substantially cut because of the lower solution vapor pressure resulting from the increased solids content.

The use of chemical additives did not significantly affect solution electrical resistance, since only relatively minute quantities could be added to the plating solution in order to maintain the low stress levels required for precision electroforming.

The results of this phase of the study indicated the inadvisability of grossly modifying the plating bath composition to control solution temperature. A more efficient bath cooling appeared as a better temperature control means for the large-scale process. This work is described in a later section. The importance of good temperature control increased when the laboratory study established that the aluminum-fiber composite is detrimentally affected by deposition from a plating solution operated substantially above ambient temperature. Plain aluminum electroforms were not so affected.

Anode Design - A prime source of solids contaminations in the plating bath is the aluminum anode which dissolves during the electroforming operation. To eliminate this problem, potential non-consumable anode materials were investigated.

A number of candidate materials were employed as anodes in the plating solution. Of the tested anodes, at low potential, +6VDC, only lead showed any sign of corrosion. At +15VDC, all tested materials experienced some anodic corrosion. The data are listed in Table 1.

Tantalum, which lost 0.16 weight per cent, was the best. Scaled-up runs with a non-consumable tantalum anode were not encouraging. The poor electrical conductivity of tantalum resulted in anode overheating which ultimately degraded the anode. Plating efficiency was considerably lowered.

A commercially available platinum-coated titanium screen, used in other plating operations, was not suitable as an anode material in the aluminum plating bath. The platinum coating was porous, which resulted in titanium contamination of the bath. Titanium build-up in the bath prevents aluminum deposition.

The more practical approach proved to be better bagging of the anode. Candidate materials for bagging were initially evaluated in the laboratory filter, since exposure to pressurized solution provided a more stringent test. A more suitable filter material was also needed.

Polypropylene felt showed considerable resistance to solution attack and could be utilized for anode bagging in the filter and as a resilient pad for the glass mold assembly rack. Ultimately, this material was utilized in the pilot cell only as a resilient pad where its exposure was limited to a static plating solution since a tendency of the felt to shred was noted in the laboratory cell.

Different types of glass cloth were evaluated next since the material was totally inert and only the weave and number of layers required needed to be established. The flexibility of the glass cloth for bagging was another consideration. An extremely close weave glass cloth provided the best containment of

foreign matter and was deemed excellent for anode bagging. This material was then used in the pilot cell, for anode bagging and as a filter pad.

The anode compartmenting approach was tried and abandoned. The more complex compartments did not retain anode slime any better than plain bagging. However, in conjunction with fiber and hollow sphere incorporation into the aluminum deposit, anode compartmenting did have advantages. This is discussed in detail in a later section.

Cell Geometry - The effect of plating tank cell geometry on fiber and microsphere incorporation was evaluated. The co-deposition process was successfully scaled-up from an initial one liter bath to two liters and four liters in the laboratory and ultimately to the 200 gallon pilot cell. Plating tank geometry varied from rectangular, square and circular. The electroforming operating conditions remained predictable during these scale-ups. Dispersion of the hollow microspheres and fibers in the large plating bath, described below, was the prime concern.

Solution Agitation - Good agitation is mandatory in aluminum electroforming. Furthermore, electroforming of fiber and/or microsphere aluminum composites requires agitation to keep those materials in suspension for successful co-deposition.

A magnetic stirrer, sufficient for plain aluminum deposition, is inadequate for co-deposition of fibers above 2 liter volumes. The effect of agitation in the laboratory cell was evaluated by utilizing a high speed explosion-proof mixing motor in the glove box.

Results may be summarized as follows:

- a) Increased agitation yielded a more uniform distribution of fibers and hollow sphere and less treeing of the deposit.
- b) Excessive agitation caused "washing away" of the fibers from the electroform surface.
- c) Non-incorporated fibers were aluminum plated as occurs in a barrel plating operation.

Agitation is controllable in the pilot cell within wide limits by throttling the filter pump and by adjusting the mold rotation speed.

Solution Filtration - The impurities present in the aluminum plating bath after its preparation derive from the formation of insoluble anode products and from insoluble impurities in the constituent chemicals. A good filtration system is mandatory. Failure to remove the impurities from the solutions results in a rough, nodular and brittle deposit. The modules show through to the front of the deposit as craters, an orange peel-like surface, and holes. Therefore, it was necessary to improve the original intermittent filtration system developed under NAS 1-3309 to provide better filtering and get continuous action. The latter task will be described in the Equipment Study section.

Improved filtration was achieved in the laboratory cell using a diatomaceous earth filter bed over a fritted glass plate. This filter removed all suspended impurities and was not quickly plugged. However, because of the large surface area required for the 200 gallon bath, this could not be incorporated into the existing pilot cell filters. Comparable solution clean-up was obtained utilizing close weave glass cloth. Unfortunately, in the pilot cell, this filter cloth was quickly clogged and required continuous attendance for dismantling, cleaning, and repacking.

Chemical Additives - Methyl borate, an additive recommended in the literature (Ref. 2) to achieve smooth, nodule-free deposits performed particularly unsatisfactorily. Bath life was reduced, and stressed aluminum deposits resulted. The large amount of gelatinous precipitation which forms, reportedly in Ref. 2, does not interfere with plating. This apparently applies to a static system.

Other additives (i.e. several amines, etc.) likewise proved unsatisfactory. Accordingly, major emphasis was directed to improved filtration and agitation techniques to minimize nodule formation.

Periodic Reverse Cycle - The electromechanical current reversal timers, used on contract NAS 1-3309 were unavailable initially during the early laboratory investigations. Deposits obtained when using substitute conventional current reversal units, were all laminated, indicating the criticality of the time delay cycles. Coherent aluminum deposits were obtained once more with the electro-mechanical timers. A plating/deplating time cycle of 190/10 seconds after an initial two hours of straight plating, yielded comparatively smooth, nodule-free deposits.

As work progressed in the strengthening of deposits study, it became apparent that the current reverse cycle would have to be eliminated. This was necessary because the silver coating on the microballoons or fibers deplate if they touch the anode. Compartmenting of the anode overcame this problem for straight plating. However, when the mold was made anodic (as in the current reverse cycle), the silver coating on microspheres or fibers, in contact with the mold, was deplated. The resulting composite lacked continuity between the specific inclusion and aluminum matrix, and was weakened rather than strengthened.

#### Masking Materials Study

Polyethylene, which was in the past regarded a suitable masking material, showed definite degradation in continuous use under actual plating conditions. Accordingly, its future use was restricted to "one-shot" applications. The attack on the polyethylene was accompanied by deposition of dark grey, nodular, "muddy" aluminum. It is now believed that constituents leaching out of the polyethylene shield in the back of the master were largely responsible for the rough, grey electroforms obtained in the pilot cell under the previous contract, NAS 1-3309.

Molded unplasticized polyvinyl chloride (PVC), exposed to the plating bath over a prolonged period, showed no signs of attack nor leaching out of detrimental impurities. Therefore, it was chosen as the rack and masking material for the pilot cell. Extruded sections, such as PVC pipe, which were also required for pilot cell components, were evaluated also. The total weight loss, after a sustained 14-day plating solution exposure did not further affect these specimens. Several extruded sections are now part of the pilot cell.

### Master Studies

Properties of the master peculiar to electroforming aluminum concentrators in the pilot cell were investigated in the laboratory using small scale models. Study areas were as follows:

Preliminary Master Materials Study - The initial efforts were directed to extend our master preparation techniques to glass substrates. This work started well; the replication achieved was excellent. The optical surface of the aluminum electroform was void-free and without evidence of plating solution attack, because a truly continuous conductive silver coating was achieved prior to electroforming.

The deposition of an adherent, stable, continuous, electrically conductive film is a prerequisite for electroplating upon a glass substrate, much more so than in the case for metal substrates where it serves only as a parting layer. Several methods (i.e. chemical reduction, vacuum deposition, etc.) were investigated. Chemical reduction, with its many advantages such as no major equipment requirement, comparative low cost, applicability to large sizes and varied geometry, low stress condition and ease of touch-up, received first consideration. Work proceeded initially with chemically-reduced silver.

Glass microscope slides, 2-inch x 3-inch, were used as substrates for this early work. The glass surfaces were thoroughly cleaned with mild alkaline cleaner, sensitized with a stannous chloride solution and then silver coated by chemical reduction of silver from an ammoniacal solution. The silvered surfaces were highly reflective and yielded excellent replications in aluminum. By controlling the composition of the surface activation solution, separation could be effected at the glass-silver interface. However the silver surface was subject to tarnishing so that an alternate coating was sought.

A recently announced chemically-reduced gold solution was investigated. A gold coating comparable in quality to the silver was never achieved. Informed of our difficulties in applying a suitable gold film, the vendor acknowledged that the process does not work well with glass substrates.

After considerable experimentation, a modification of the chemically-reduced gold application techniques was found which permitted deposition of an apparently sound gold film on which aluminum could be electroformed. Adhesion of aluminum to the gold layer was excellent. However, the gold film was highly stressed and

had only mediocre adhesion to the glass substrate. Also sufficient thickness to achieve an impervious gold coating could not be built up. Build-up of an impervious coating by deposition of a flash layer had to be restricted to acid-type gold plating baths because cyanide gold lifted up the initial layer. The resulting combination was generally poor. Because of the inconsistencies and inadequacies of the gold coating, further work on this approach stopped.

Subsequently, vacuum deposited gold films on glass were investigated. These were continuous although very thin. Initial results were encouraging, but since the gold film was easily scratched and was difficult to touch-up during seating of the cove-forming ring on the glass substrate, an appreciable coating buildup would be mandatory. Thick vacuum deposited films are generally highly stressed so that once more a flash coating was required. As such, this approach was abandoned.

Techniques for spray application of a continuous, adherent and conducting chemically-reduced silver film on glass, were established in the lab. Materials and fixtures to duplicate this procedure for scaled-up runs with the 30-inch glass master were secured and assembled in the pilot cell.

Separation Techniques Study - Successful separation of a 30-inch electroformed aluminum mirror with cove ring required total integrity of the deposit. The advantages of building up an initial heavy (up to 0.001 inch) flash coating prior to placement of the cove ring will be developed in the following section.

The chemically-reduced silver provided an excellent parting layer between the electroform and the glass substrate. By modifying the composition of the surface activation solution and the initial plating/deplating conditions, separation could be effected at the glass-silver or the silver flash (see below) - aluminum interface. This latter control enabled electroforming an all-aluminum mirror from a silver flash deposit required for cove ring attachment. This is described in detail below.

Torus Attachment Study - In the previous contract, NAS 1-3309, a transition ring mold was affixed to the male nickel master. This extended the mirror electroform to include a cove ring to which a torus was attached for structural support. The transition ring mold-male nickel master interface was a knife edge joint. The excellent throwing power of the plating solution resulted in the aluminum depositing under the knife edge instead of merely bridging over. Therefore a notch or fault line appeared in all electroforms. This was inherently a point of weakness creating problems in separation of the mirror from the master and in usage.

A different approach was now developed and tested in the laboratory study. A cove ring, with knife edge, was grown-into the electroform deposit. Subsequently a torus ring was attached to the cove ring for structural support and attachment of the electroformed concentrator.

In the laboratory, a prototype grow-in cove ring was affixed to a watch glass, Figure 9, simulating conditions anticipated in the pilot cell. The knife edge of the cove ring scratched the conductive film on the glass and thereby destroyed the continuity of the electroform. Proper placement of the knife edge of the cove ring on the glass required a "heavy" initial coat to prevent any damage to the conductive film. The use of a nickel flash permitted proper ring placement and prevented solution seepage under the optical surface. However, if left on, the nickel surface would negate one of the objectives of aluminum mirror, i.e. providing a non-magnetic metal mirror. A silver or aluminum flash coating was deemed the more useful approach to achieve total separation or adhesion, as required.

Techniques for obtaining maximum adhesion of the aluminum electroform to electrodeposits of silver and of aluminum, were evaluated in the laboratory cell. Procedures were established for obtaining excellent adhesion of the aluminum deposit to an initial silver flash. Good adhesion was also obtained to an initial aluminum flash by combining a current reverse cycle and a substrate pretreatment procedure. Procedures for effecting separation at the silver-aluminum or aluminum-aluminum interface were easily developed by decreasing the oleic acid activating solution concentration.

Fixturing was procured to handle either candidate flash coating for the pilot cell and the choice was left open.

#### Strengthening of Deposits Study

Methods for improving the mechanical properties of electroformed aluminum deposits by the incorporation of fibers and hollow microspheres were investigated. The feasibility of the process had already been demonstrated in work performed by the General Electric Company. This study was directed toward developing processing techniques suitable for large scale use.

It was realized that glass fibers and hollow silica microspheres would not provide high absolute values of strength. On the other hand, the process developed for the incorporation of glass fibers and silica microspheres can later be modified for other reinforcing materials. Glass fibers and hollow microspheres were readily available, inexpensive, and thus were well suited for experimentation.

Fiber and Microsphere Surface Preparation - Milled glass fibers were coated by chemically reducing silver on the fiber surface to obtain a sound matrix-fiber interface bond. Initially, the adhering impurities over the large surface area of the fine glass fibers in the plating bath substantially decreased its useful life. Tight process control later eliminated contamination of the plating solution.

The procedure consists of first sensitizing a batch of fibers or spheres with a stannous chloride solution. After several washings with demineralized water, these materials were coated with a silver film formed by the chemical reduction of an ammonical silver solution at about 50°F. The low temperature slowed the reaction rate sufficiently so that the fibers or microspheres could be filtered from the solution before insoluble contaminants were formed. The fibers (or microspheres) were thoroughly rinsed to remove any adhering silver solution. Moisture removal was effected by flash evaporation using a vacuum pump and desiccator. Silvered spheres, prepared in this manner, were free-flowing and ready for addition to the electroforming bath. The identically prepared silvered glass fibers required screening prior to addition to the plating solution and, like the silvered microspheres, did not cause chemical reaction and degradation of the bath. In comparison, in case of addition containing normally negligible moisture (i.e. adding make-up anhydrous ether, containing a maximum of 0.08% water) reaction with the hydride is always noted.

Microsphere and Fiber-Aluminum Co-Deposition - The one liter glass fiber-containing plating bath was scaled-up successively to two liters, then to four liters. This study established that in the current reverse cycle the silvered fibers deplated, destroying the fiber matrix bond, which thereby nullified the strengthening effect of the fibers. Therefore, current reversal was omitted in subsequent process studies. Contact of the silvered fibers with the anode (even with increased bagging) had a like effect but to a lesser extent. Compartmenting of the anode provided a satisfactory solution without unduly increasing the plating bath resistance. This was incorporated into the pilot cell design.

It was further determined that the initial thickness of silver on the fiber surface greatly affected the strength of the electroformed co-deposit. Accordingly, a "heavy" deposit of silver was thereafter applied to microspheres and fibers by several successive applications of the silvering solution.

In an initial series of runs, silvered silica spheres were co-deposited with aluminum over an electroformed nickel substrate. The aluminum electroform was still quite ductile. Inclusion of foreign particles into an electroform normally causes surface roughness, nodular growths and treeing. This was barely evidenced in our composite. Microscopic examination of the front and rear surface and of the cross-section confirmed the integrity of the deposit.

In other runs a mixture of glass fibers and microspheres were co-deposited simultaneously with aluminum. The electroform was examined, using a metallographic microscope, and the sound inclusion of fibers and microspheres was noted.

An initial sample for test was prepared with low quantity fiber loading, primarily due to no fiber addition to the bath in the overnight segment of the one-day run. The initial results were encouraging. The character of the deposit



was excellent, comparable to previous samples. Although a truly high strength electroform had not yet been achieved, the increase in strength was regarded as significant. Work continued toward process improvement with greater fiber loadings of the aluminum deposits. The effect of current density was concurrently investigated.

At the conclusion of the laboratory study, technique improvements in incorporating glass fibers resulted in increases in UTS and yield point of 87% and 115%, respectively, as compared with plain electroformed aluminum. These data appear in Table 2. Additional physical property data are presented in Appendix A.

It should be noted that the increased strength of these electroforms have been achieved with comparatively light loadings of fibers. This is shown clearly in Figure 10, a photomicrograph of a glass fiber-incorporated aluminum electroform. The fiber alignment within the plane of the electroform, noted since the early stages of this work, is visible in the photomicrograph.

With round-the-clock operation of the pilot cell during the fiber-aluminum electroforming run, fibers were added throughout the run. Thus, when the co-deposition parameters are firmly established for the scaled-up pilot cell, even greater increased strength electroforms can be reasonably anticipated than have been achieved in the laboratory, where fiber loadings are made during the daytime segment of each run.

Test specimens prepared with microsphere incorporation also showed increased mechanical strength. Ultimate tensile strength was increased 37% (to 15,100 psi vs 11,050 psi). These data are listed in Table 3. Also see Appendix A.

The spherical character of the microspheres presented no orientation problem as exists with fiber incorporation. This factor plus directly applicable experience with fiber incorporation accounts for the excellent results obtained above.

Our work demonstrated that technique improvements with incorporation of one material yield data applicable to other similar material.

A cursory look was taken at the incorporation of conductive materials into the aluminum matrix. Iron powder, 0.0003 inch diameter tungsten wire in 1/8 inch lengths and short length (several mm) nickel fibers were utilized. Data for the incorporated-electroformed aluminum specimens appear in Table 4. No effort was made at optimization, beyond feasibility demonstration. This work demonstrated that all manner of materials can be incorporated into the aluminum matrix. Thus, the really high strength materials (i.e. boron, silicon carbide, carbon filaments, etc.) offer the opportunity for increased strength aluminum electroforms of practical significance.

## EQUIPMENT STUDY

The equipment study was directed toward improvements in the pilot cell fabricated under NASA Contract NAS 1-3309 and towards preliminary design of an electroforming cell for handling up to 10 feet diameter solar concentrators.

### Pilot Cell Modification

Design modifications to various pilot cell systems were evaluated and specific features incorporated into the pilot cell.

Filtration System - An effective filtration system has emerged as a prerequisite for electroforming sound, nodule-free aluminum electroforms. The present requirements of continuous agitation to keep the hollow spheres or fibers in suspension made necessary revamping the previous semi-continuous filtration system. Design modifications of the filtration system, as fabricated under Contract NAS 1-3309, which would utilize the two existing filters, were evaluated.

An intensive search for a suitable self priming pump, to replace the high/low pressure cycle in the filter, yielded one vendor who would guarantee its performance with the ethereal plating solution. (Note - On the previous contract no such vendor guarantee could be secured]. To keep down the cost, the pump was sized for the existing filters utilizing the filter membrane established in the laboratory for the pilot cell. A better system, shown in Figure 11 and 12, should filter approximately 200 gallons per hour.

The effective filtration area of the existing filters is too low for the 200 gallon aluminum plating solution. The result was frequent clogging of the filter membrane necessitating opening the filters for cleanout and membrane replacement. In addition to interrupting filter-agitation of the plating solution, each opening was a potential source of solution contamination thus shortening bath life.

In the laboratory cell, the plating solution was filtered through a bed of diatomaceous earth supported on a fritted glass plate. The large surface area of the diatomaceous earth gave the filter a long life and the solution was effectively cleaned up. Unfortunately this could not be incorporated into the existing filters, primarily because of potential passage of the diatomaceous earth into the 200 gallon bath and availability of only up to 9-inch diameter fragile fritted glass plates. Also, the surface area/solution ratio, while improved would still be far from satisfactory. As such, a system of tubular cartridges involving a major redesign or scraping of the filters is indicated. This is described in a following section.

Cathode Rotation System - Cathode rotation was found to be highly desirable to insure a uniform deposition. A number of possible methods for a direct-drive cathode were evaluated. The resulting design incorporated into the pilot cell rack is shown in Figure 13. Criteria were to obtain a smooth continuous motion to avoid jolting the glass mold, easy accessibility to the gas-driven motor for maintenance, rugged construction and not requiring rotary seals through the plating tank wall. Rotary speed was adjustable by controlling the inlet gas pressure and flow rate.

This system proved highly satisfactory throughout the pilot cell runs. Also, our gas consumption dropped to a fraction of the previous pilot cell gas requirements.

Quick-Entry of Mold into Tank - In the first pilot cell, the mold was lowered into the plating solution by a hand-operated winch. The result was a slow, jerky motion into the bath with potential horizontal striations on the optical surface caused by the momentary halts in lowering the mold. Rapid controllable entry into the plating solution was accomplished by installing an explosion-proof motor with a drive mechanism to the existing glove box winch, as shown in Figures 14 and 15. This functioned as designed in pilot cell operation eliminating this previously major problem.

Purge Gas Venting System - The purge gas venting system on the pilot cell used to plug-up repeatedly during runs, because sublimed  $\text{AlCl}_3$  from the plating solution collected in restrictive sections of the vent lines. This resulted in hazardous overpressurization of the cell. The proximity of the purge gas inlet and vent lines presented problems in an inadequate purge, also. Modification of the filtration system, etc., necessitated reworking portions of the gas purge system. This was all corrected in conjunction with setting up the pilot cell in General Electric's "D" Street facility.

Plating Solution Cooling System - Modification of the plating bath composition, etc., as a passive means of controlling solution temperature was evaluated in the laboratory cell. As described earlier, this line of investigation was fruitless. Accordingly, improved solution cooling was indicated.

The water coils, which were bonded to the front and rear face of the plating tank, were removed and water jackets were welded in their place as shown in Figure 16. It was determined that sufficient cooling surface now existed if a chilled water supply was used. A water cooling tower at "D" Street provided the required cooling water. In pilot cell electroforming runs, the plating solution could be maintained at room temperature.

Fiber Feed System - A hopper through which fibers and microspheres can be added to the plating bath was incorporated into the filtration system. The filters were by-passed during addition of fibers, etc., and for agitation of the plating solution, as required, to maintain suspension of the fibers or microspheres. The system, shown in Figure 17, worked out well in the pilot cell and brought a high concentration of fibers or microspheres directly to the mold.

## Large Electroforming Cell - Preliminary Design

Design requirements for handling and electroforming large (10 feet diameter) solar concentrators were investigated and a preliminary design was developed. This preliminary design fell into specific categories listed below.

Plating Cell - The plating cell, Figure 18, demonstrates one improved design over the present pilot cell. A conforming anode seated on the tank bottom keeps anode impurities away from the horizontal mold positioned above. A machined metal mold, feasible now from a cost basis because of computerized milling machines, would be used. The filter return line would discharge plating solution onto the mold face. The air lock assembly (top portion) contains a lifting device for raising and lowering the mold in the plating tank. A bevel gear drive will rotate the mold during plating. A submersible pump will be used in conjunction with the filtration system. Figure 19 shows another plating cell design adapted for fiber co-deposition.

Filtration System - The critical requirement of an adequate efficient filtration system has been discussed previously. A number of filter element cartridges, which markedly increase the filtration surface area, have been incorporated into a new filter design. This appears in Figure 20. The resulting design should give excellent solution clean-up and require a minimum of opening of the system for filter element replacement.

Concentrator Structural Support - Figure 21 presents a number of alternate designs for attaching structural support members to the electroformed solar concentrator. The first choice is for growing-in a prepared torus-cove ring combination to fabricate potential flight hardware.

Separation Fixture - Vacuum separation, deemed particularly important for large size electroforms, is achieved by utilizing the airlock portion of the plating cell as the vacuum chamber. This is shown in Figure 22. Dual use of this component enables cost and space savings for the unit.

## CONCENTRATOR FABRICATION

### Master Fabrication

A male paraboloidal glass mold was fabricated as per contractual requirements. Specifications were for a rim angle between  $45^{\circ}$  and  $60^{\circ}$  with a surface finish of two microinches rms or less and having surface angular errors of less than two minutes over 95% of the area.

Twelve vendors were sent specifications of the optical requirements, as defined in Contract NAS 1-5743, for a glass, convex, paraboloidal mold. The order was placed with the Farrand Optical Company because of their fine reputation, low bid, and promised quick delivery. Mold dimensions are shown in Figure 23. The focal length was 16.8 inches, corresponding to a  $48^{\circ}$  rim angle, well within the

45° to 60° contractual limits. The selected rim angle with its minimum depth paraboloid provided greater plating tank room.

The mold was inspected using the optical ray trace equipment used on contract NAS 1-4105 (See Ref. 3). All measurements were within the minimum readability of the instrument ( $5\frac{1}{2}$  arc seconds) indicating the high geometric accuracy of the ground glass mold. Photographs made by reflecting light from the mold surface lacked sufficient contrast for evaluation due to the inherent low reflectivity of uncoated glass. Visual inspection of mold surface reflections on the darkened room walls indicated that the surface quality was good.

### Electroforming Concentrators

Concentrator fabrication was accomplished in the modified pilot cell. Details of the operating procedure are presented in Appendix B and results of an optical inspection of one concentrator model are presented in Appendix C.

An initial "shakedown" aluminum electroforming run was performed in the modified pilot cell using a surplus 12-inch diameter paraboloidal nickel mold. The run was a total success and demonstrated the following:

1. All component modifications, etc., functioned as planned without difficulties.
2. The aluminum plating solution, prepared on the previous contract, NAS 1-3309, deposited good aluminum. This proved that degradation did not occur even after 30 months of combined use and storage of the plating solution. Earlier literature data indicated a bath life of less than a year.
3. The aluminum electroform replicated the master surface extremely well.

Because of the good quality of the deposit, decision was made to depart from the original plan and attempt to electroform a 30" mirror in this aged solution. Accordingly, all preparations were made for the first electroforming run using the 30-inch diameter glass mold.

30-Inch Mirror No. 1 - The 30-inch glass master surface was cleaned, sensitized by a  $\text{SnCl}_2$  solution and coated with a chemically-reduced silver film. A thin (0.001 inch) silver flash electrodeposit was applied and the grow-in cove ring was mounted over the master. The mold was then immersed in the aluminum plating solution and an aluminum concentrator was electroformed.

The glass mold, with the adhering aluminum electroform was removed from the plating solution. An aluminum torus ring was bonded to the cove ring grow-in for structural support. A thin polyurethane foamed-in-place backing was applied to the non-optical concentrator surface to permit evaluation of this rigidizing technique. Separation was accomplished although the following difficulties appeared:

1. A lamination in the electroformed deposit was discovered. The thickness of the initial layer indicated this occurred between two and three hours after start-up. This could not be correlated with power failure, power fluctuation, or any other occurrence. The age of the solution did not appear to play any role in the lamination. Where the laminate was not lifted away from the bulk deposit of the mirror (about 70% of the surface area), the electroform appeared to be the best surface and geometry to date.
2. The mirror was cut up to permit thorough examination of the lamination. It was found that in reality, not one, but several laminations occurred within the aluminum, and also the silvered parting layer was loose.

The cause of this failure was finally traced to our filter purging procedure. Each time the filter clogged up, the residual solution in the filter was transferred back into the plating tank prior to opening the filter. Nitrogen gas pressure was used for the transfer of the solution and for purging the filter. The gas bubbles swept the cathode surface and passivated it.

No further aluminum lamination occurred after the purging procedure was changed, since the filters were now emptied into the storage tank.

3. A number of cracks in the glass mold were noted after separation. Several of these were chip-like although still firmly adhering to the mold. All cracks ran circumferentially and were restricted to two to three inches from the mold's periphery. Farrand Optical Company, fabricator of the glass mold, sent one of their experts with over 30 years experience to look at the mold. He could not offer any explanation but stated that the average life of a glass mold is only a few electroforming runs because of stresses in the glass and that a first-time breakage is quite common. He suggested several approaches to make the mold serviceable for additional runs. These were evaluated and it was found that filling the cracks with "colloidal silver" paste would render the mold usable once again.

30-Inch Mirror No. 2 - After filling the cracks with colloidal silver, the excess was wiped off and feathered in. The "old" solution was replaced with freshly prepared solution as a precautionary measure, before the failure mode of the previous run was understood.

Processing was identical to the previous run and the aluminum concentrator was electroformed over a silver flash. An aluminum torus was bonded to the cover ring grow-in for structural support. Separation was accomplished without difficulty in a vacuum chamber, with the following items noted:

1. The overall geometry and specularity of the mirror was only fair.

2. While there was no lamination within the aluminum deposit, the adhesion of the aluminum electroform to the silver flash was weak at the periphery, good further in. Conditions in the pilot cell were comparable to those in the laboratory cell where good adhesion could always be obtained. To attain better adhesion at the periphery, a high initial potential was planned for the next run.
3. No additional damage to the mold was noted.

30-Inch Mirror No. 3 - Preparations were made for another run. The cracks were refilled with fresh colloidal silver to prevent potential electroform hang-up. Processing was as for Mirror No. 2 but with an initial higher plating potential. An aluminum torus was bonded to the grow-in cove ring and the mirror was separated from the glass mold. The following was observed:

1. The overall geometry and specularity of the mirror was fair.
2. Adhesion of the electroform to the silver flash improved at the periphery and remained good further in. The adhesion techniques were re-investigated in the laboratory cell. Improved adhesion was achieved employing a reverse current with a time delay cycle initially before aluminum deposition. This was scheduled for the next run.
3. No additional damage to the mold was noted.

30-Inch Mirror No. 4 - Preparations proceeded as with the previous run, employing an initial reverse cycle before aluminum deposition. After the start of aluminum plating, periodic additions of silvered glass fibers were introduced into the plating bath. Co-deposition of aluminum and glass fibers proceeded as per techniques developed in the laboratory cell. An aluminum torus was bonded to the cove ring and the mirror was separated from the glass mold. The following observations were made:

1. The overall geometry and specularity of the mirror was good.
2. Adhesion of aluminum electroform to the silver flash appears improved but is still not strong. During this period a still better technique for adhesion to the silver flash was developed in the laboratory. This was scheduled for the next run.
3. At the vacuum deposition vendor, who processed these mirrors in a proprietary manner, the silver flash parted entirely. The aluminum electroform still showed good geometry.
4. No additional damage to the glass mold was noted.

30-Inch Mirror No. 5 - Preparations proceeded as with the previous run. To attain maximum adhesion, the mold was lowered into the plating bath with electrical power on. All glass fibers were filtered from the plating solution prior to the run. Periodic additions of silvered hollow silica microspheres were made to the plating bath. Co-deposition of aluminum and microspheres proceeded throughout the run.

The efficiency of the pilot cell co-deposition technique as compared with the laboratory cell was indicated in the higher-than-planned hollow sphere loading. (Estimated from depletion, at 40g microspheres in the mirror). On removal from the plating bath the electroform, still on the mold, experienced a thermal shock in the cold plating room. Several cracks in the electroform developed before our eyes within minutes. This was particularly unfortunate because adhesion to the silver flash was excellent and could not be torn apart and because the surface was devoid of "orange peel".

30-Inch Mirror No. 6 - The above run was repeated using a much reduced microsphere concentration. All operating conditions were as before with one major difference. Since a pilot cell proven adhesion technique has been established, it was decided to make an all aluminum mirror by separating at the silver-aluminum interface. Mirror separation was effected as planned and the following was observed for the mirror:

1. The overall geometry and specularity of the mirror was fair.
2. The aluminum separated completely without any hang-up on the silver surface.
3. Another crack, identical in appearance to the others, was noted near the center of the glass mold.



## CONCLUSIONS

The work described in this report was largely successful.

The aluminum electroforming process was improved by systematic elimination of the problems defined in the Final Report, NAS 1-3309. We have learned how to overcome porosity and pinholes in the deposit, bridge across gaps, make sound grow-ins, and reduce the roughness on the back of the deposits. The equipment was greatly improved. The new cooling and condensing system virtually eliminated the hitherto enormous evaporation losses. Also, the direct drive cathode rotation system and filter pump circulation cut the gas consumption to a fraction of the previous level. We have learned how to deposit over glass masters and how to retain or discard parting layers.

Some problems still await solution, mainly because the contract expired before sufficient experimental data could be secured in the pilot cell.

The most significant achievement of the present work is probably the technique of producing reinforced composites by aluminum electroforming. Here we have refined a most desirable process, which has great potential in numerous structural areas. With only three pilot cell runs and not more than a dozen laboratory runs, this composite fabrication technique cannot be said to be optimized. Indeed, from theoretical considerations, it is evident that we have barely opened the door by demonstrating the soundness of the approach in larger than laboratory sizes.

The aluminum bath has far superior throwing power than any other plating bath. Thus, occluded particles are fully encapsulated, without leaving voids. The electrical field provides partial alignment of the fibers in one plane.

Presently the best metal matrix composite fabrication processes must use a prewoven, prealigned filament system, and must work with molten metal or compacted powders. Both methods damage the fibers. Also the geometry of the fabricated components is limited. The codeposited electroform is free of such shortcomings. It is doubtful if any other plating bath or vapor/vacuum deposition process could provide throwing power comparable to the ethereal aluminum bath.

The significance of this work, thus far not completed, became apparent from the numerous inquiries received for information relating to potential structural applications for the process.

This program considerably furthered the technology of aluminum electroforming in its various aspects. The process became better controllable, the equipment is well defined, the processing cost was significantly reduced by drastically cutting material requirements. The unique theoretical and practical significance of aluminum electroforming is demonstrated in areas ranging from high strength composites to cladding and to structural parts.

T A B L E 1

ANODIC CORROSION OF SELECT MATERIALS IN ETHEREAL  
PLATING SOLUTION (3.4M  $\text{AlCl}_3$ , 0.4  $\text{LiAlH}_4$ ).  
DEPOSITION TIME PER TEST WAS 7 HOURS

<u>Specimen Material</u>	<u>Weight Change, Per Cent</u>	<u>Specimen Appearance</u>	<u>Weight Change, Per Cent</u>	<u>Specimen Appearance</u>
Copper	None	No Visible Attack	-36.2	Heavy corrosion holes formed in material
Molybdenum	None	No Visible Attack	-0.65	No Visible Attack
Brass	None	No Visible Attack	-18.6	Removable, black sur- face coating formed
Silver	None	Very Slight Tarnish	*	Removable, black sur- face coating formed
Tantalum	None	No Visible Attack	-0.16	No Visible Attack
Nickel	None	No Visible Attack	-0.51	Thin black coating formed
304 Stainless Steel	None	No Visible Attack	-0.55	Thin black coating formed
Lead	-1.4	Black, flaky coating formed	**	**
Niobium	None	No Visible Attack	-1.14	No Visible Attack

\* Specimen corroded through during run. Weight change could not be measured.  
\*\* Not tested.

T A B L E 2

EFFECT OF FIBER-INTEGRATION INTO ALUMINUM ELECTROFORMS

	<u>Glass Fiber-Incorporated Electroformed Aluminum</u>				
	<u>Electroformed Aluminum</u>	<u>Light Loading</u>	<u>Heavier Loading 20 asf</u>	<u>Increased Loading</u>	<u>Improved Processing</u>
Ultimate Tensile Strength, psi	11,050	11,050	14,320	16,296	20,700
Yield Point @0.2% Offset, psi	8,450	--	--	--	18,300
Elongation, %	Z6	(1)	(2)	12	(1)

(1) Not Measured

(2) Specimen broke in vise grip and could not be measured.

T A B L E 3

EFFECT OF SILICA MICROSPHERE-INCORPORATION INTO ALUMINUM ELECTROFORMS

	<u>Electroformed Aluminum</u>	<u>Microsphere-Incorporated Electroformed Aluminum</u>	
		<u>20 asf</u>	<u>30 asf</u>
Ultimate Tensile Strength, psi	11,050	15,100	13,380
Elongation, %	26	16.5	9.2

T A B L E 4

EFFECT OF INCORPORATING OTHER MATERIALS(\* INTO ALUMINUM ELECTROFORMS

	<u>Electroformed Aluminum</u>	<u>Electroformed Aluminum Co-deposited with:</u>		
		<u>Iron Powder</u>	<u>0.3 Mil Tungsten Wire</u>	<u>Nickel Fibers</u>
Ultimate Tensile Strength, psi	11,050	11,595	10,850	10,425
Elongation, %	26	20	7	18

- (1) Materials used were readily available and were given one initial look without the optimization of material form.



FIGURE 1 OVERVOLTAGE CURVE  
for a 3.4M  $\text{AlCl}_3$ -ether solution at 35°C

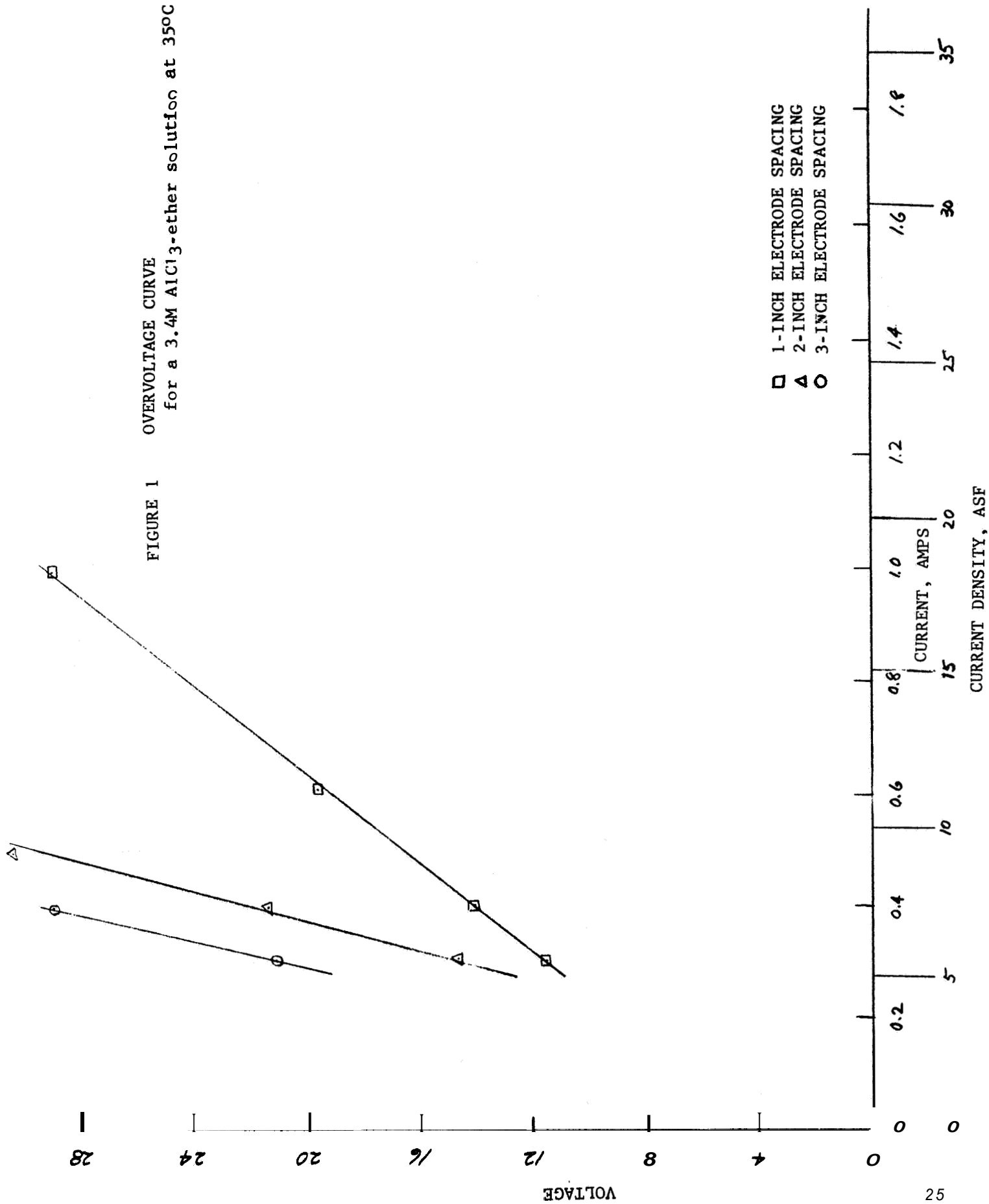


FIGURE 2 OVERVOLTAGE CURVE

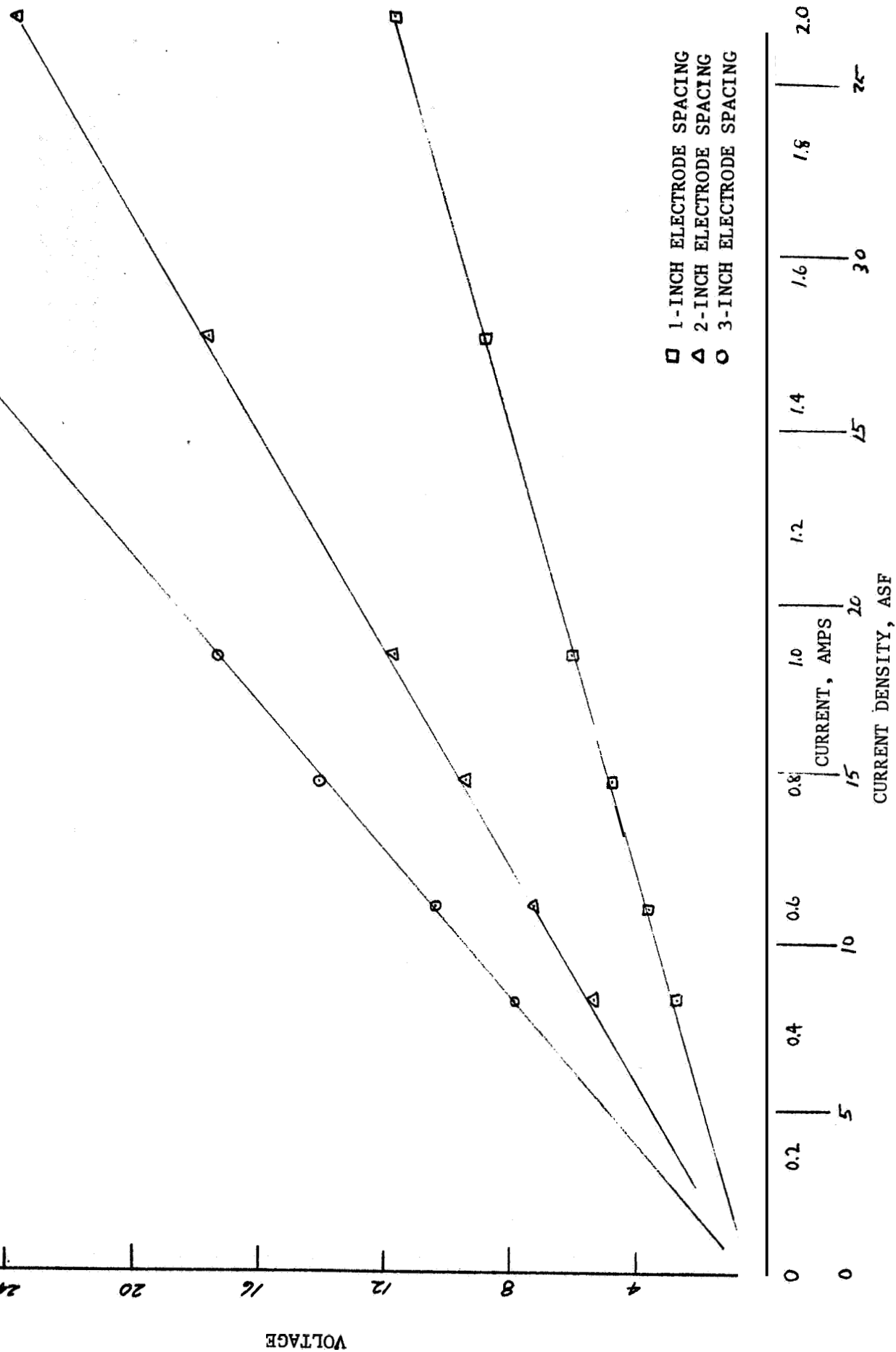
for a 3.4M  $\text{AlCl}_3$ -0.4M  $\text{LiAlH}_4$ -ether solution at 35°C

FIGURE 3 OVERVOLTAGE CURVE  
for a 3.4M  $\text{AlCl}_3$ -0.6M  $\text{LiAlX}_4$ -ether solution at 35°C

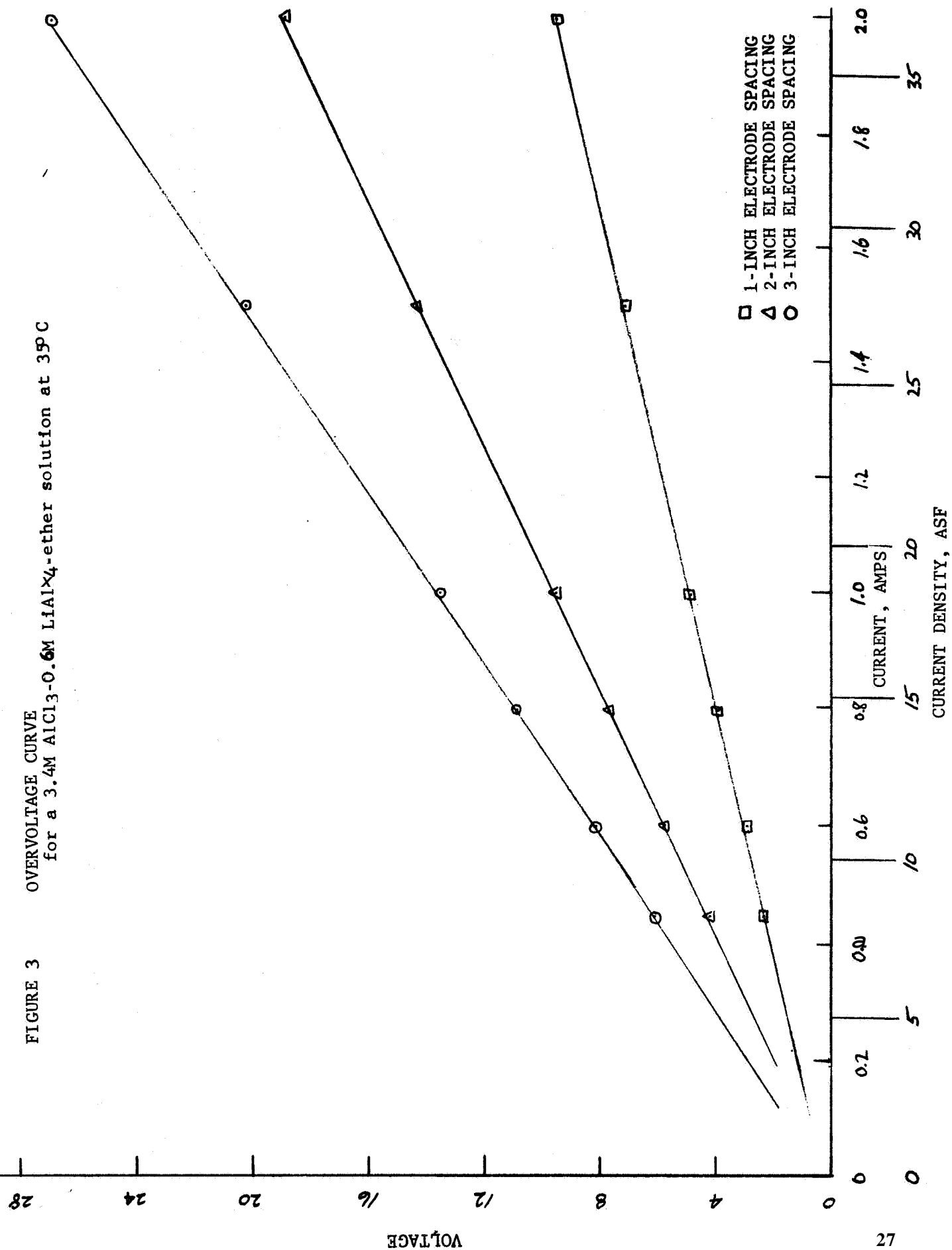




FIGURE 4 OVERVOLTAGE CURVE  
for a 3.4M  $\text{AlCl}_3$ -0.8M  $\text{LiAlH}_4$ -ether solution at 35°C

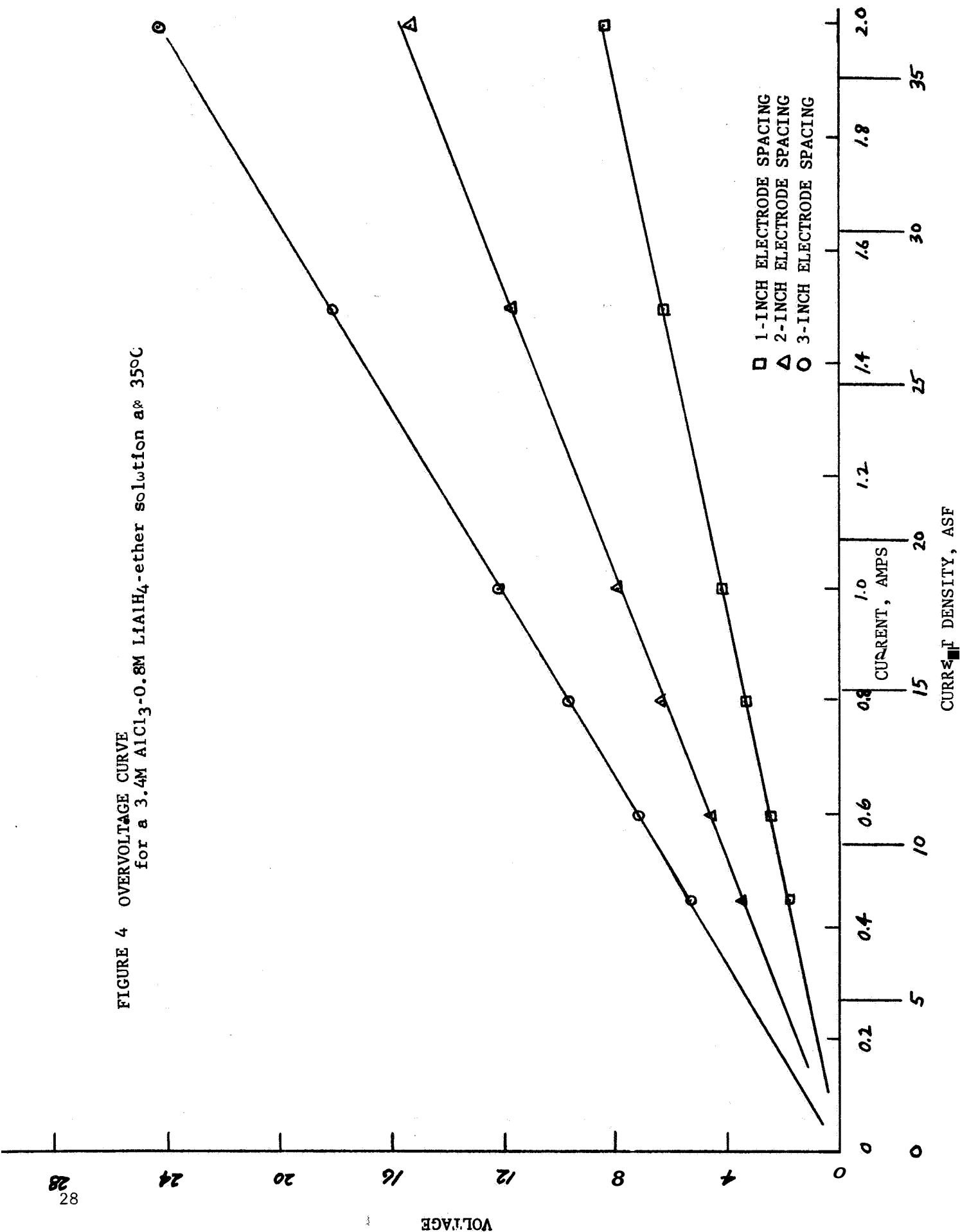


FIGURE 5 OVERVOLTAGE CURVE  
for a 3.4M  $\text{AlCl}_3$ -1.0M  $\text{LiAlH}_4$  ether solution at 35°C

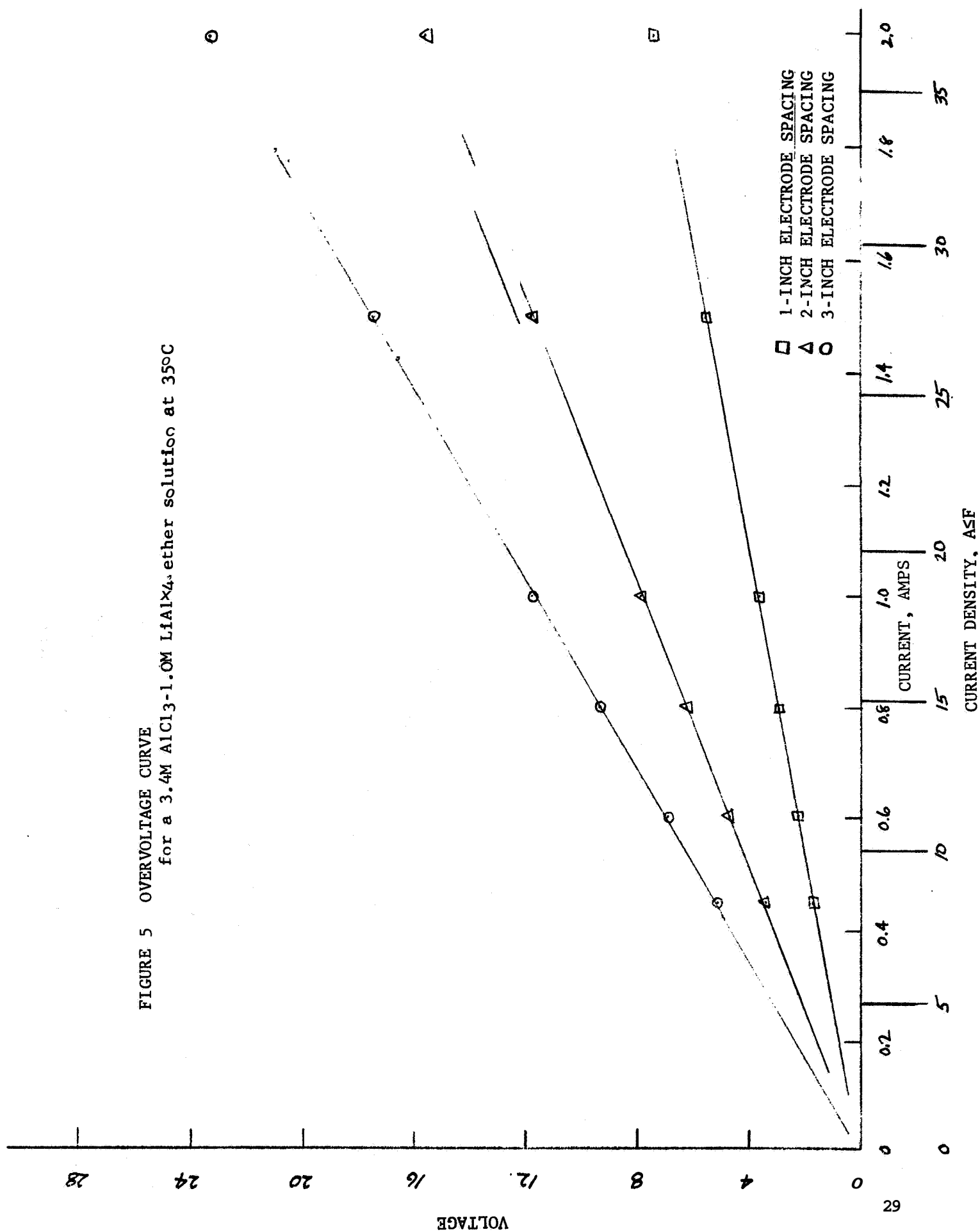


FIGURE 6 OVERVOLTAGE CURVE for a 3.4M  $\text{AlCl}_3$ -1.2M  $\text{LiAlH}_4$ -ether solution at 35°C

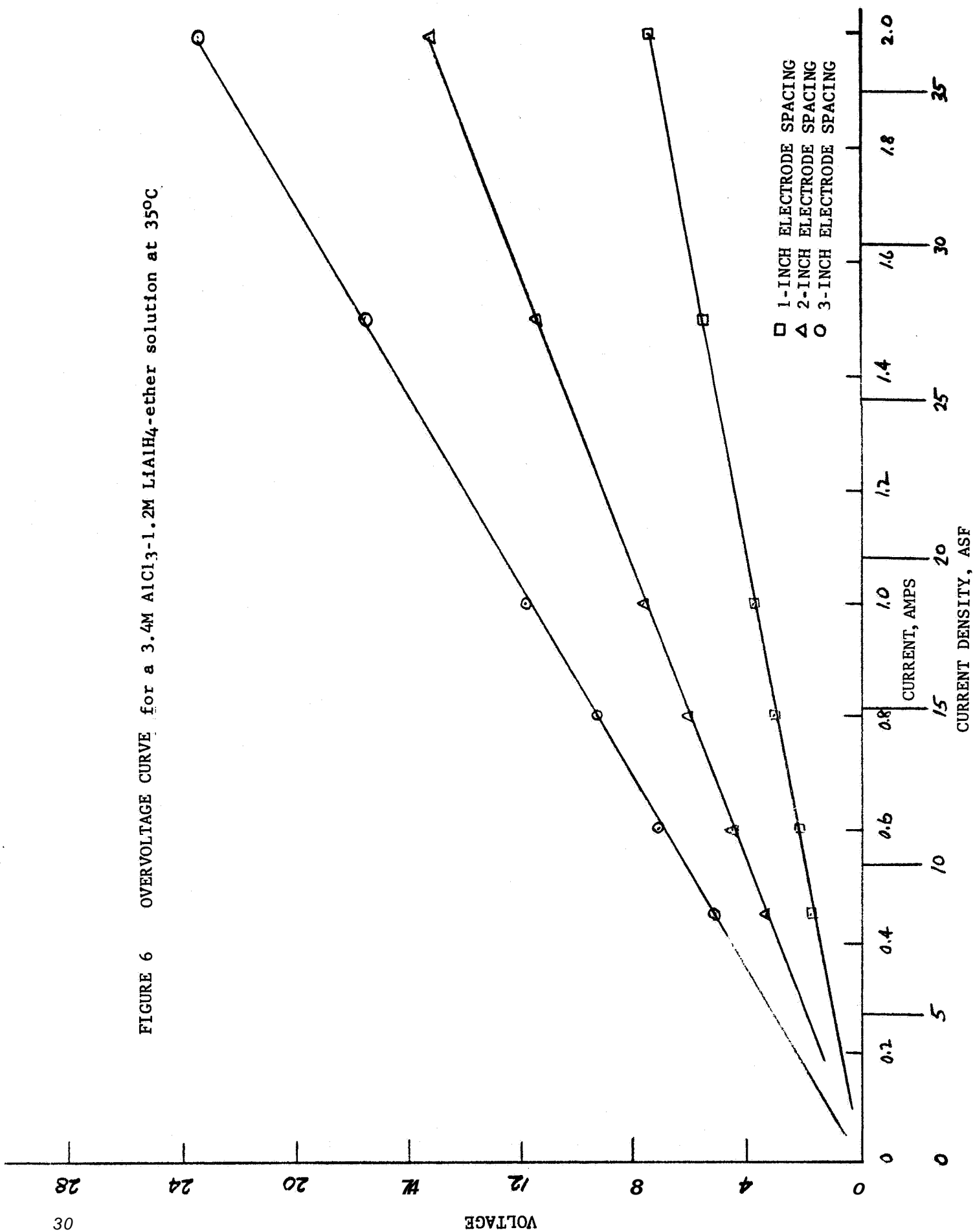


FIGURE 7 OVERVOLTAGE CURVE for a 3.4M  $\text{AlCl}_3$ -1 4M  $\text{LiAlX}_4$ -ether solution at 35°C

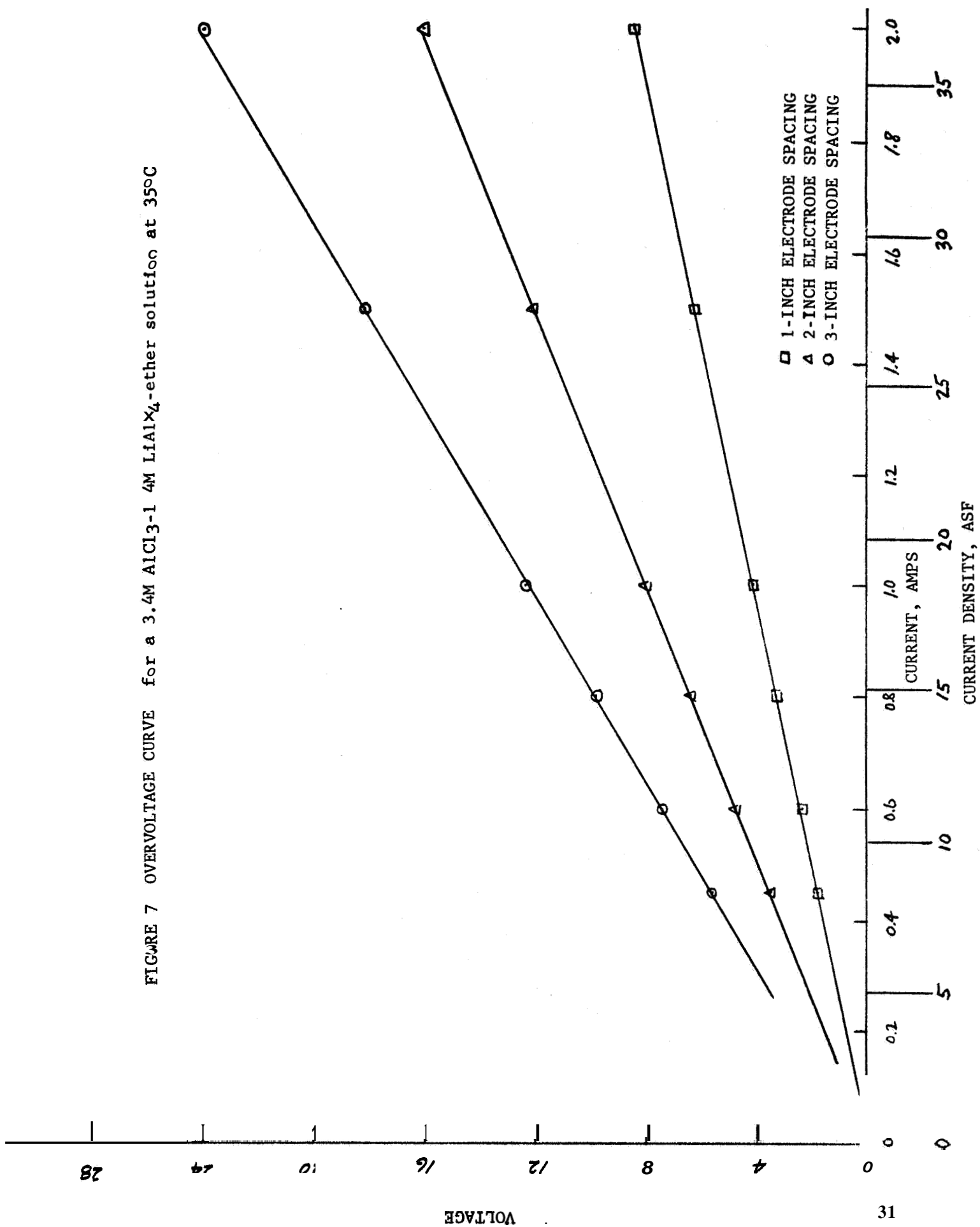
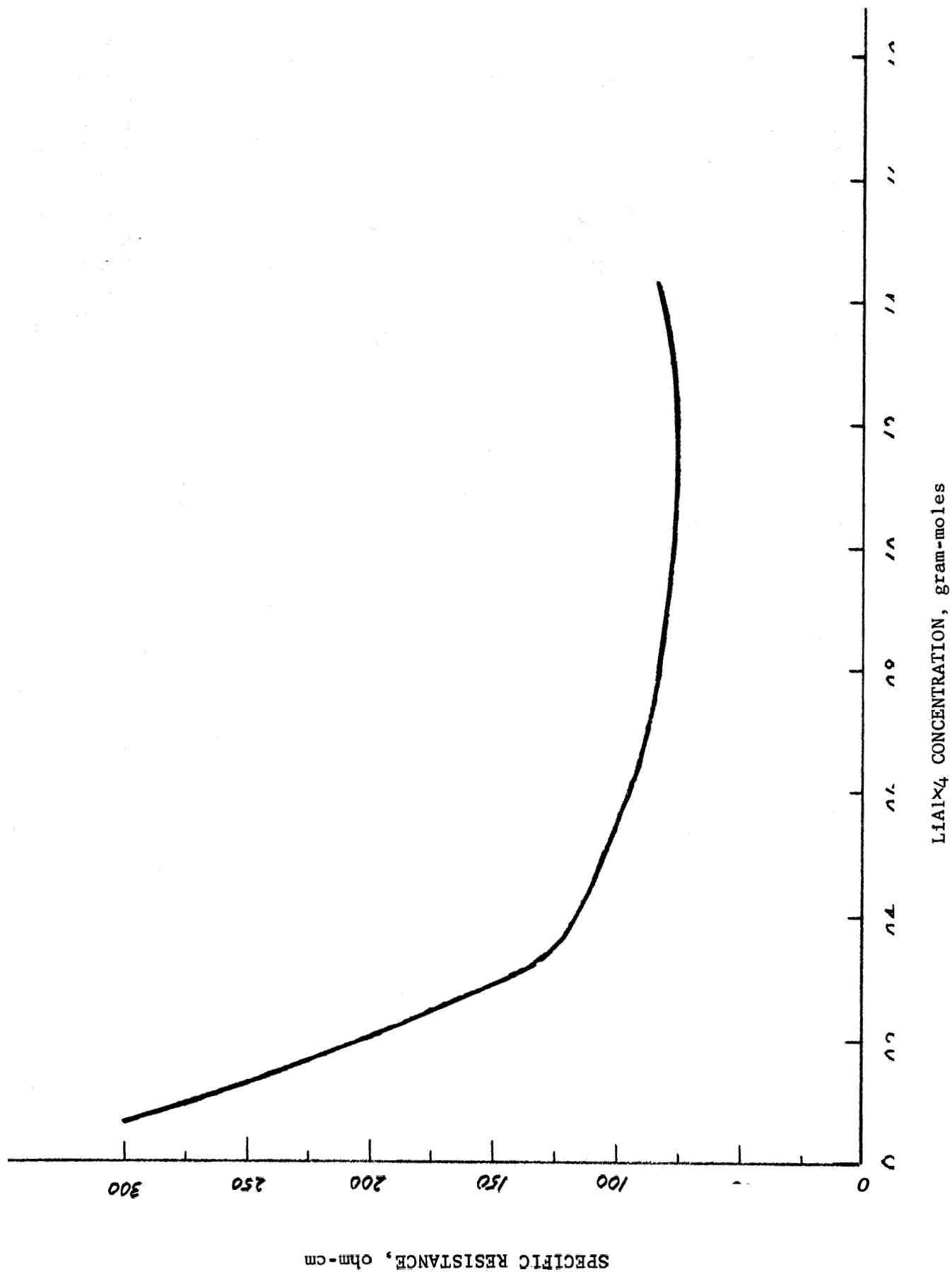


FIGURE 8 THE EFFECT OF  $\text{LiAlH}_4$  CONCENTRATION ON THE SPECIFIC RESISTANCE OF A 3.4M  $\text{AlCl}_3$ -ETHER SOLUTION AT 35°C



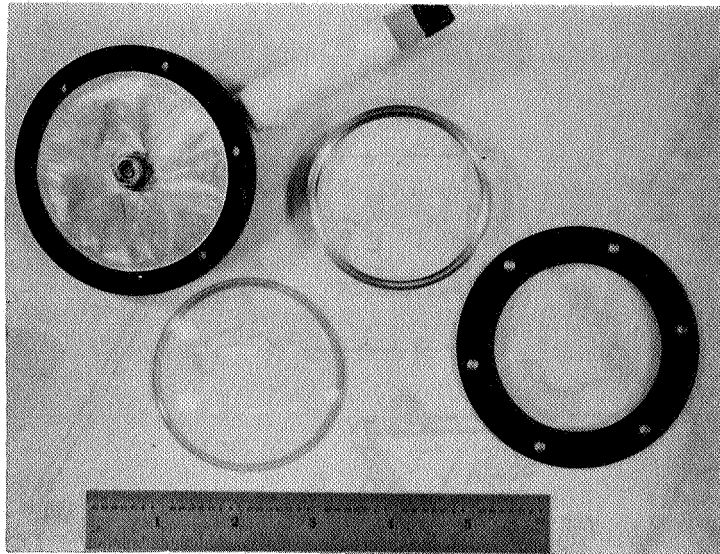


Figure 9. Laboratory rack, prototype of pilot cell rack. Components from left to right are rack, itself, watch glass (mold) aluminum cove ring grow-in and the retaining ring.

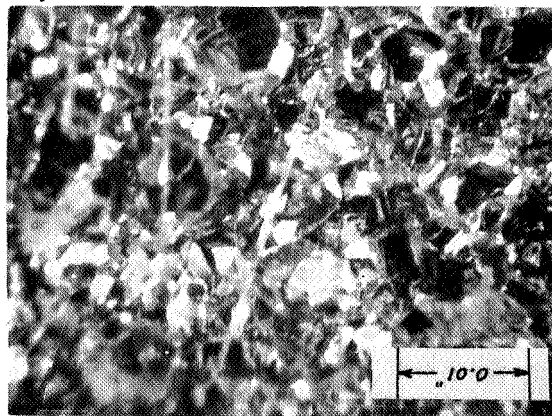
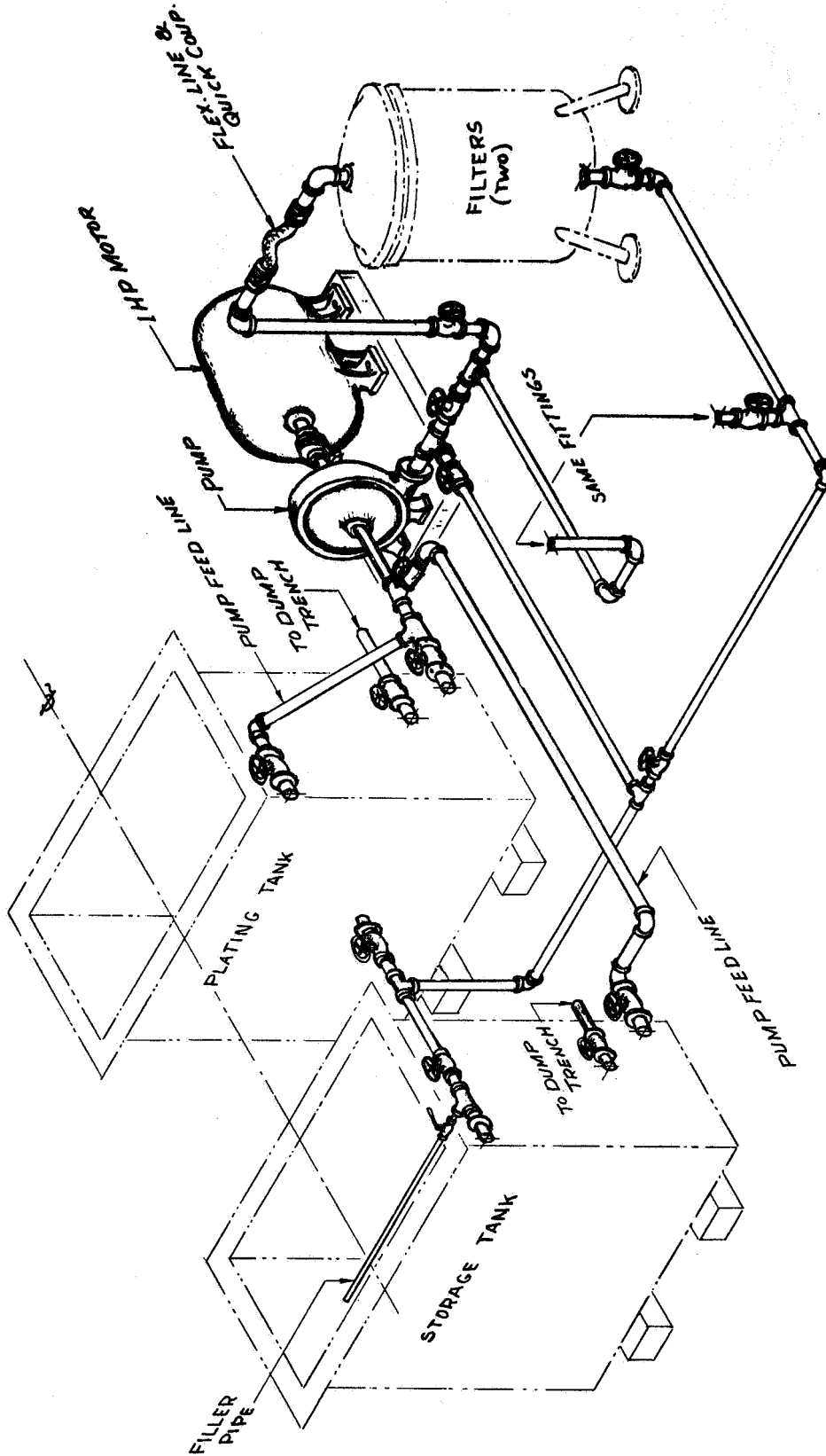


Figure 10. Photomicrograph of back face of glass fiber-incorporated aluminum electroform. The alignment and loading of glass fibers is evident.



PIPING DIAGRAM  
PILOT CELL

FIGURE 11

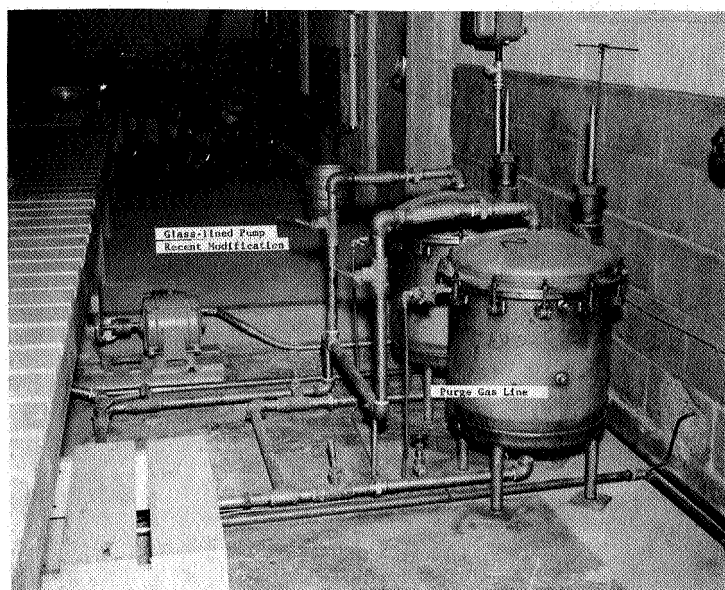


Figure 12. Close-up view of filtration system including the two filters and the recently-added glass-lined pump. Plating tank cooling water lines appear in foreground on right.

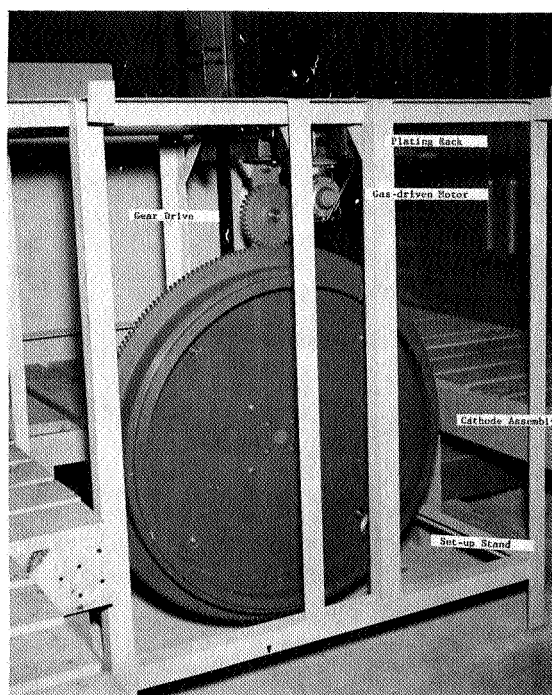


Figure 13. Close-up of mock-up stand. The rack which will hold the glass master is inside. Note the gas driven motor to drive gear which rotated mold holding rack member, as modified.



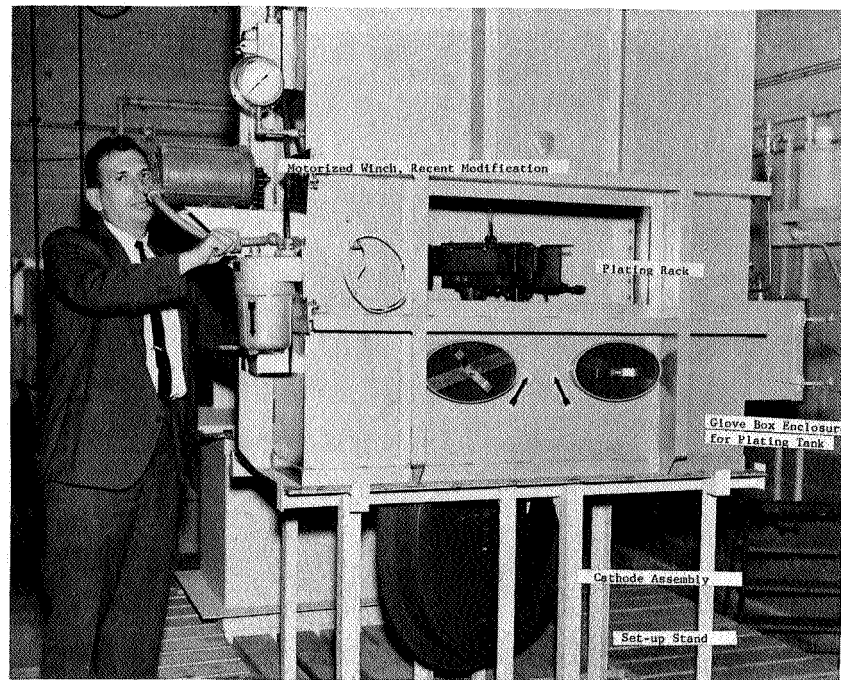


Figure 14. Hoisting the plating rack into the glove box enclosure using the motorized drive.

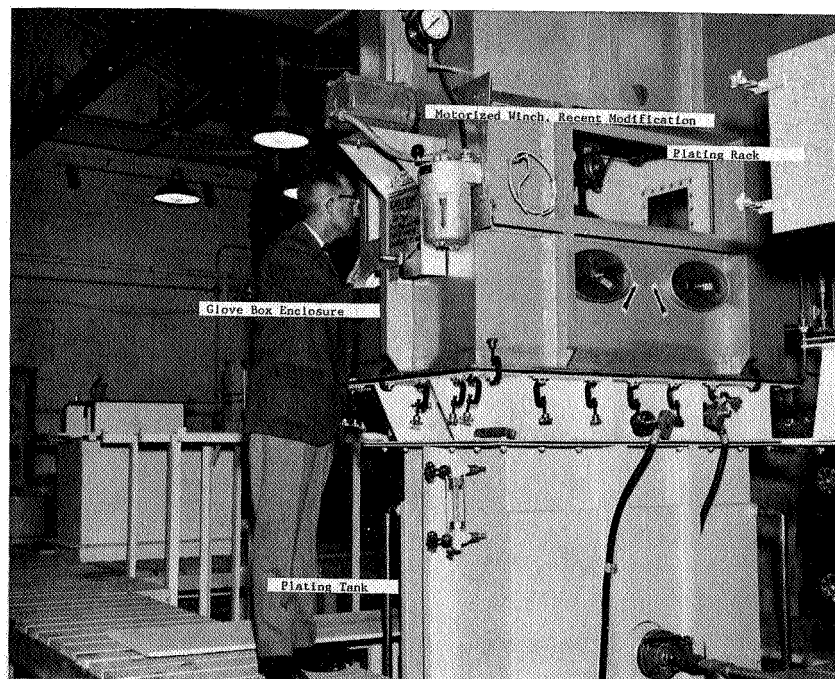


Figure 15. The glove box enclosure with plating rack inside positioned over plating tank. The motorized drive mechanism was utilized to lower the plating rack into position in the tank.

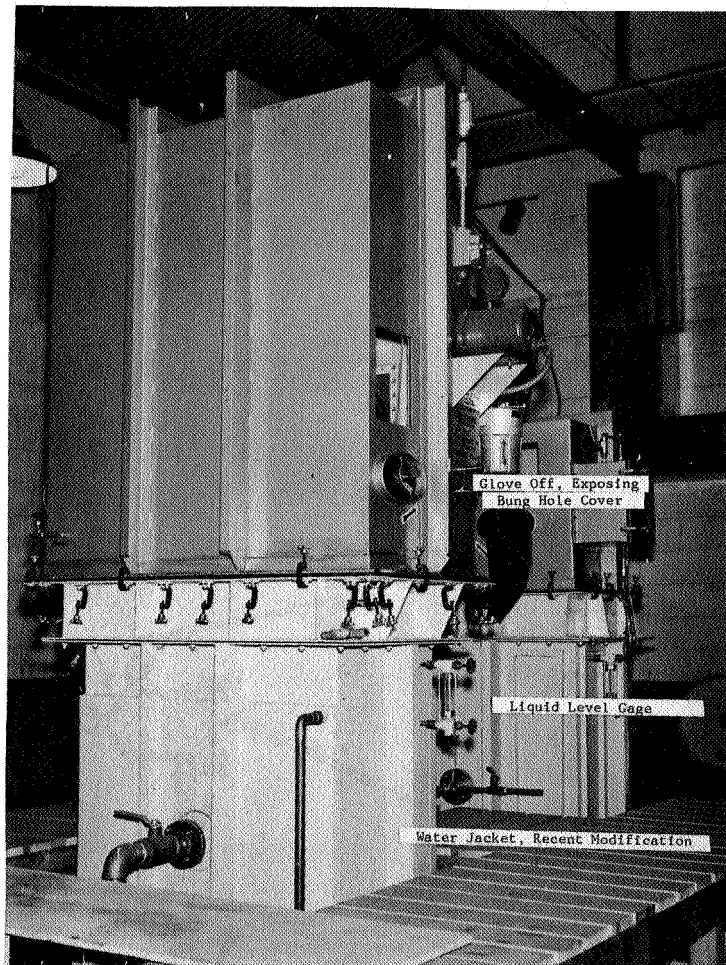
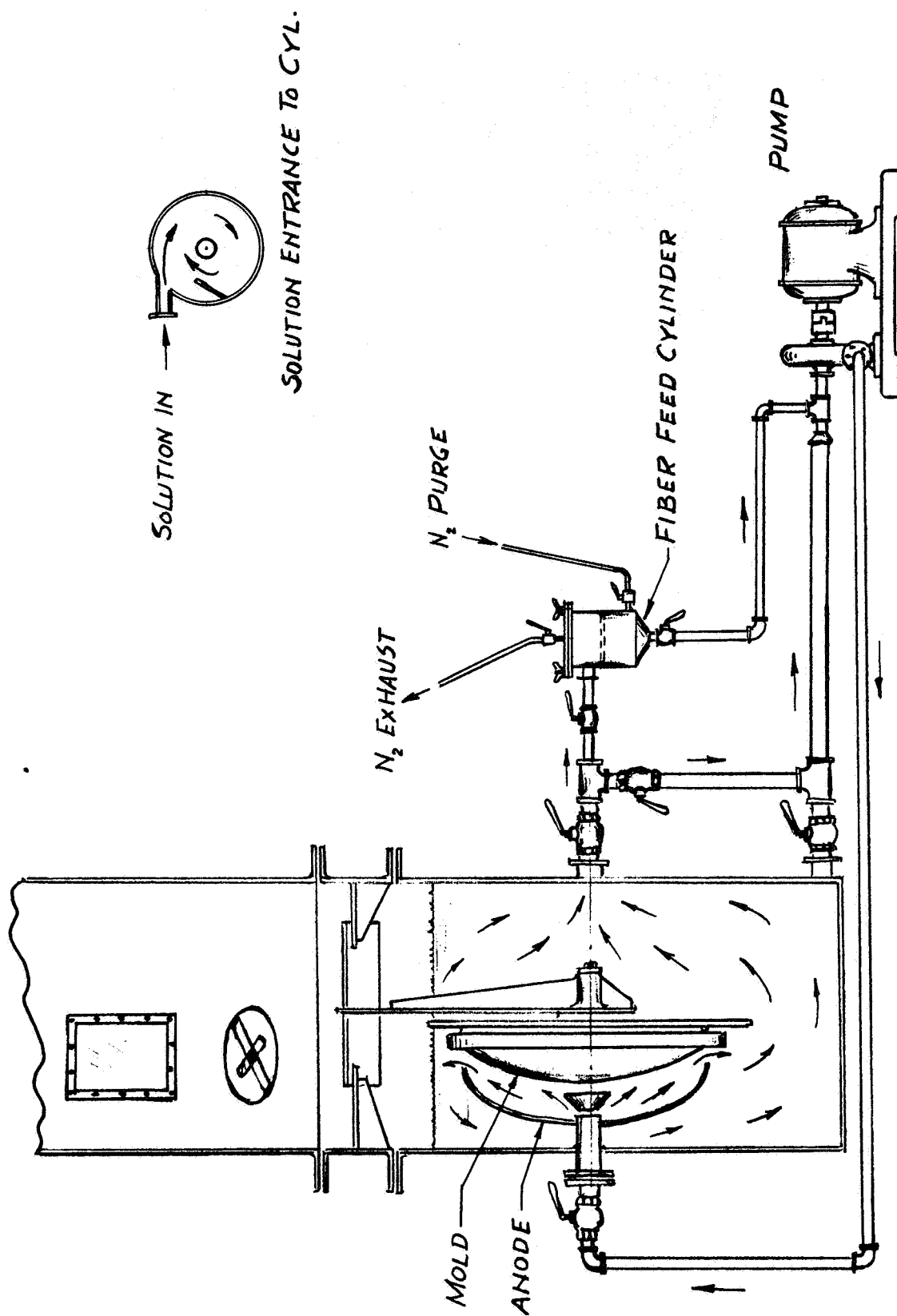


Figure 16. Close-up of rear of plating tank and glove box enclosure and of storage/mixing tank (background). Note the motorized drive (recent modification) on glove box to effect rapid entry of the mold into plating solution. Water jacket on the plating tank (another new modification) provided more efficient cooling.

FIGURE 17 FIBER/MICROSPHERE FEED SYSTEM



**FIGURE 18**  
**PRELIMINARY DESIGN OF A PROPOSED PLATING CELL**

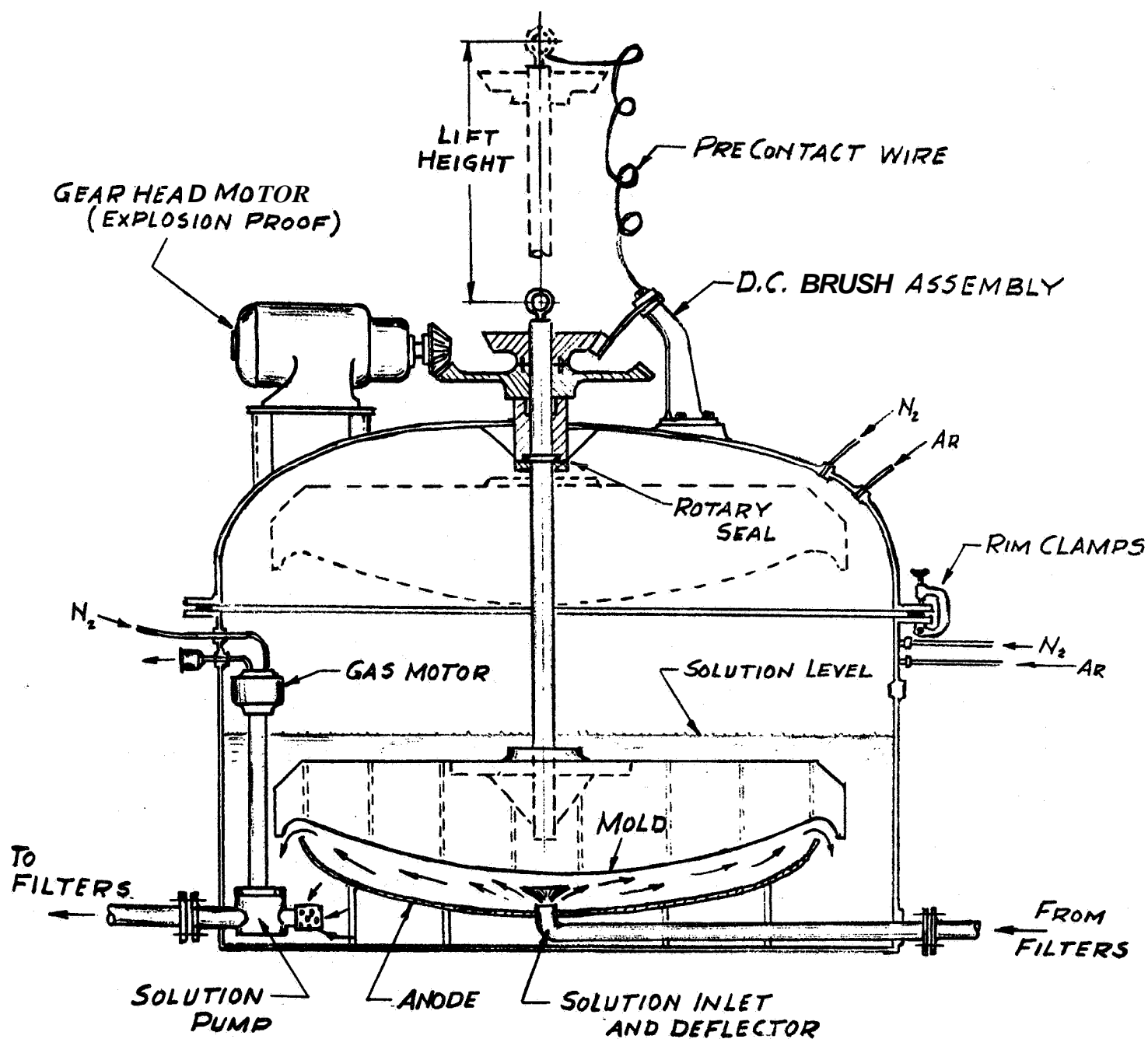


FIGURE 19

PRELIMINARY DESIGN OF A PROPOSED  
PLATING CELL FOR FIBER CODEPOSITION

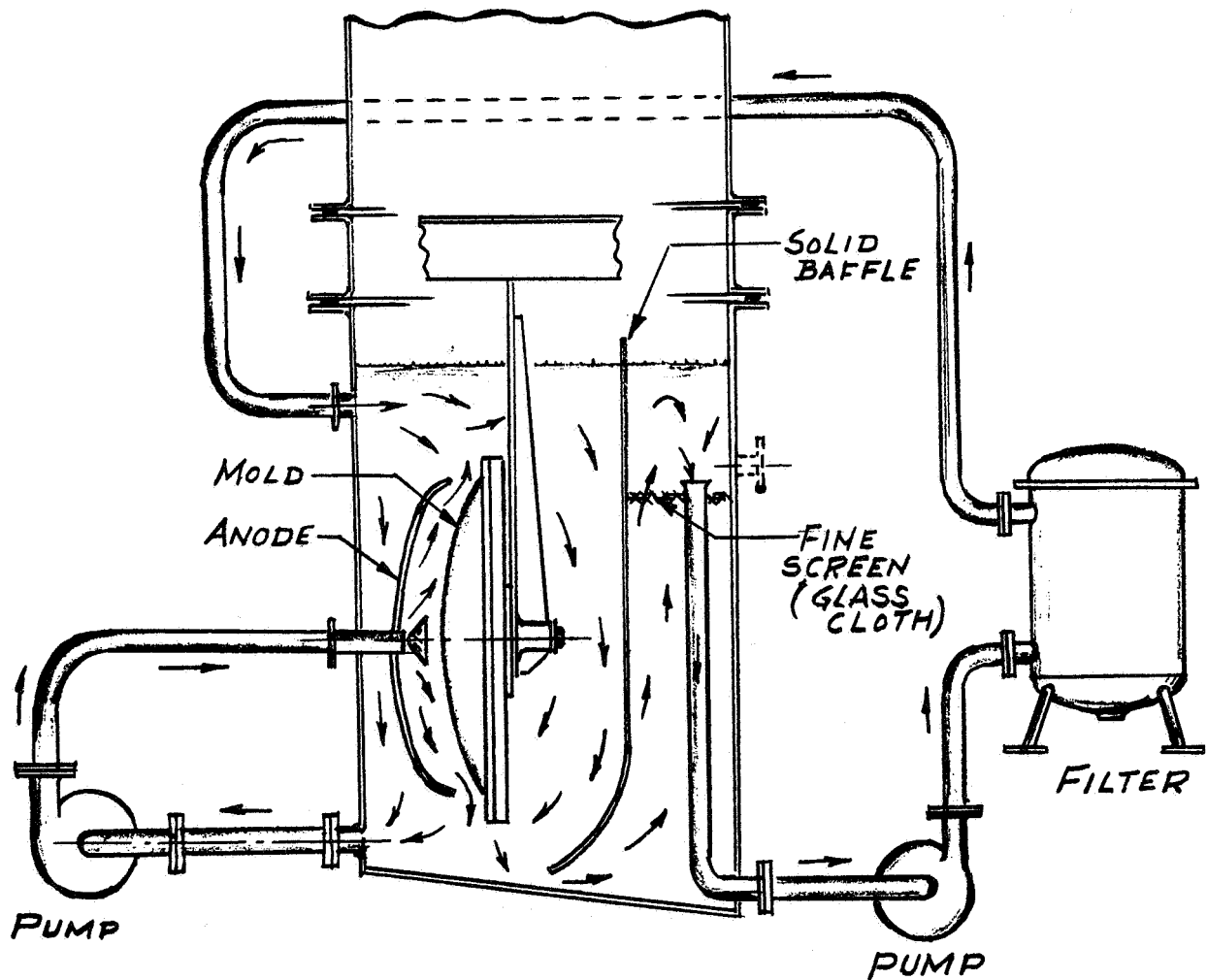
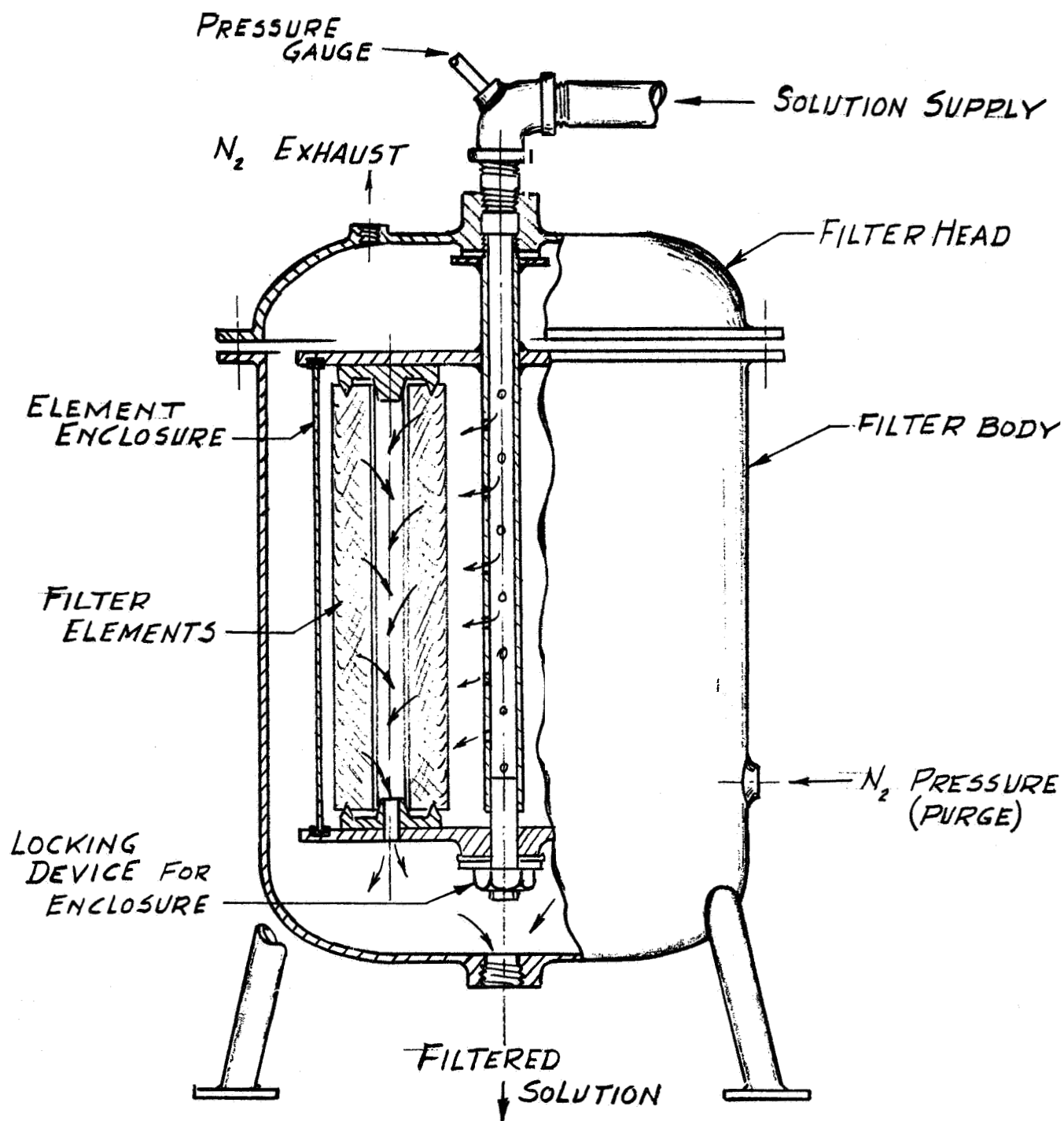
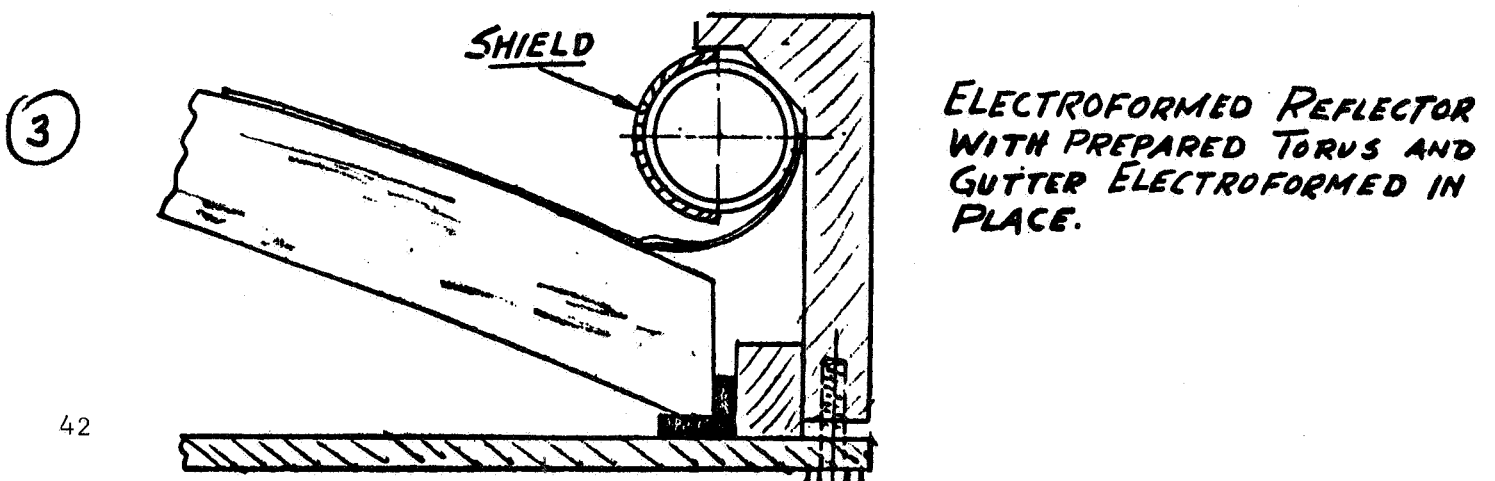
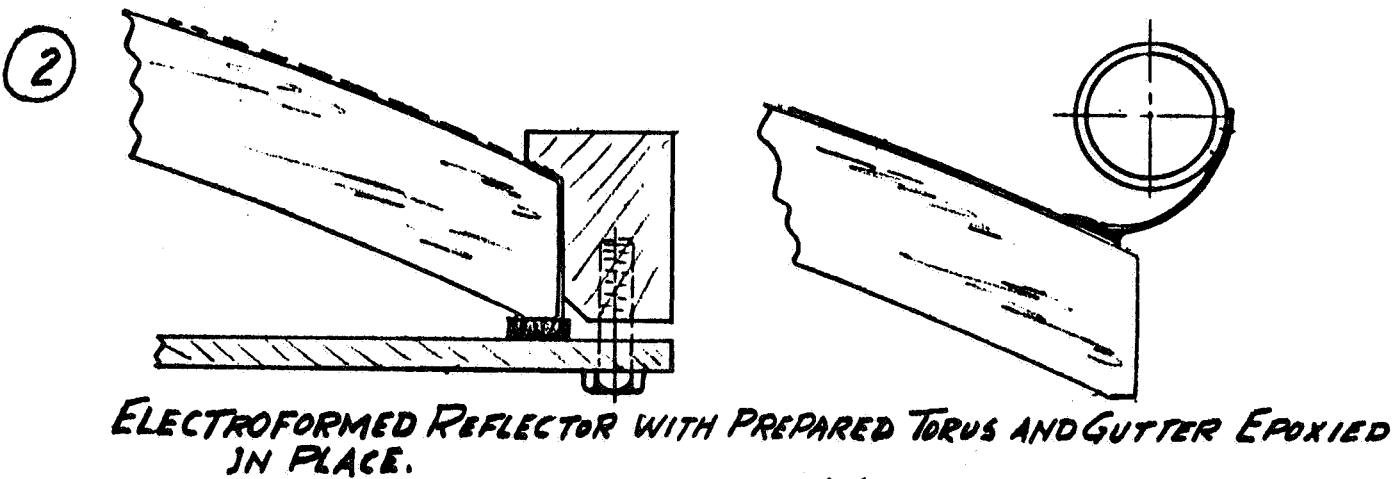
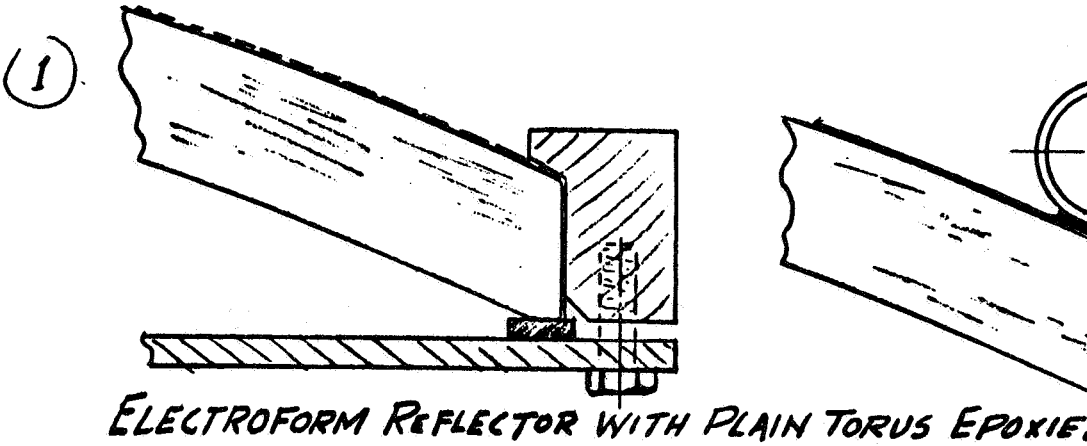
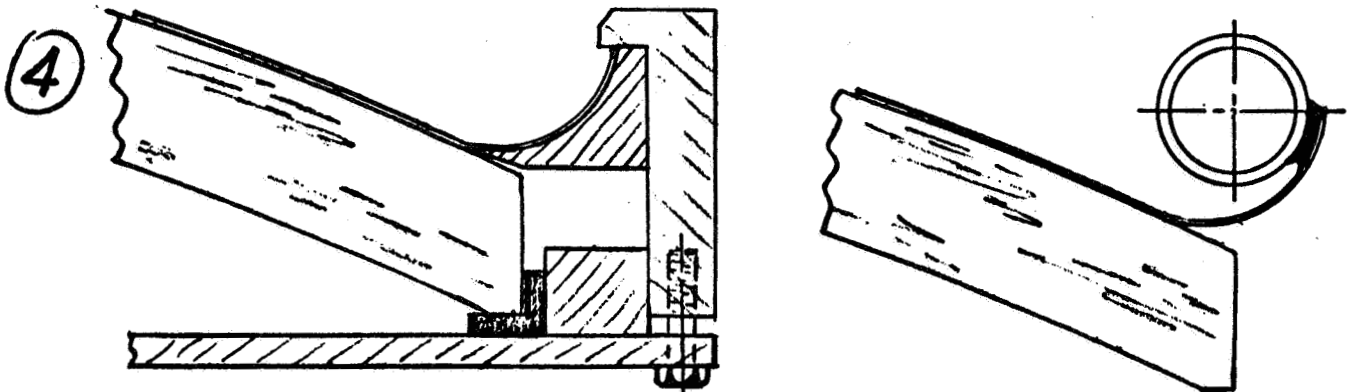


FIGURE 20  
FILTER ASSEMBLY

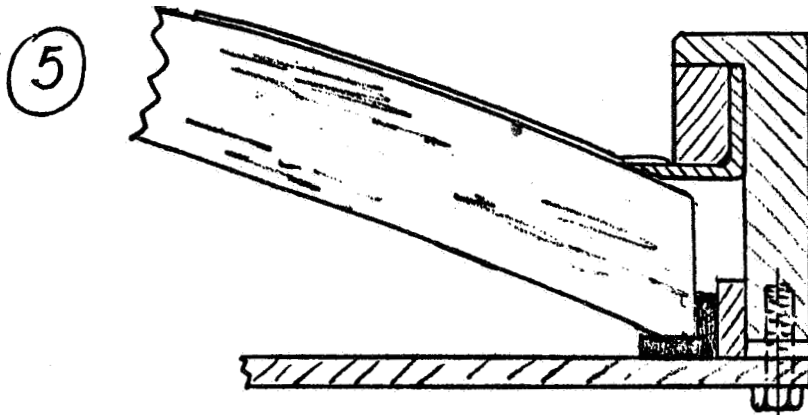




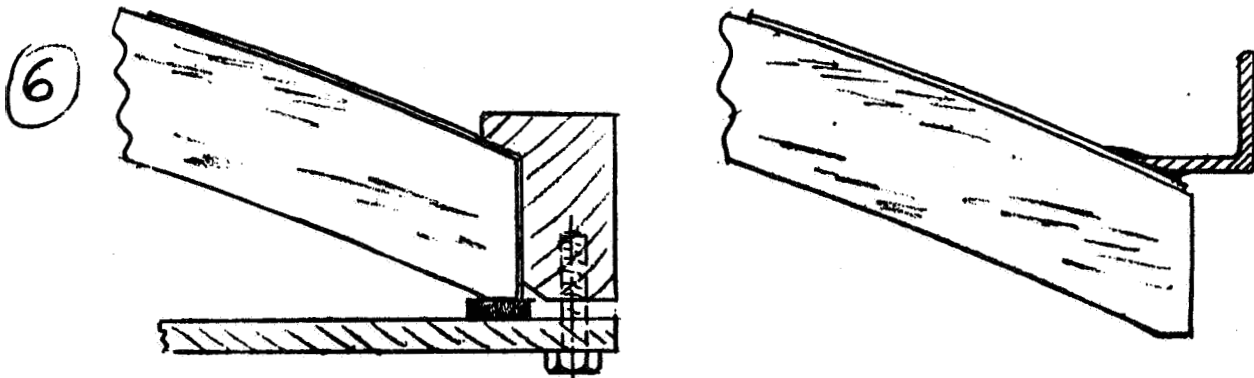
CONCENTRATOR STRUCTURAL SUPPORT



*ELECTROFORMED REFLECTOR AND GUTTER WITH TORUS EPOXIED IN PLACE.*



*ELECTROFORM REFLECTOR WITH PREPARED ANGLE RIM ELECTROFORMED IN PLACE.*



*ELECTROFORMED REFLECTOR WITH ANGLE RIM EPOXIED IN PLACE.*



FIGURE 22

VACUUM CHAMBER UTILIZING  
AIR LOCK of PROPOSED PLATING CELL

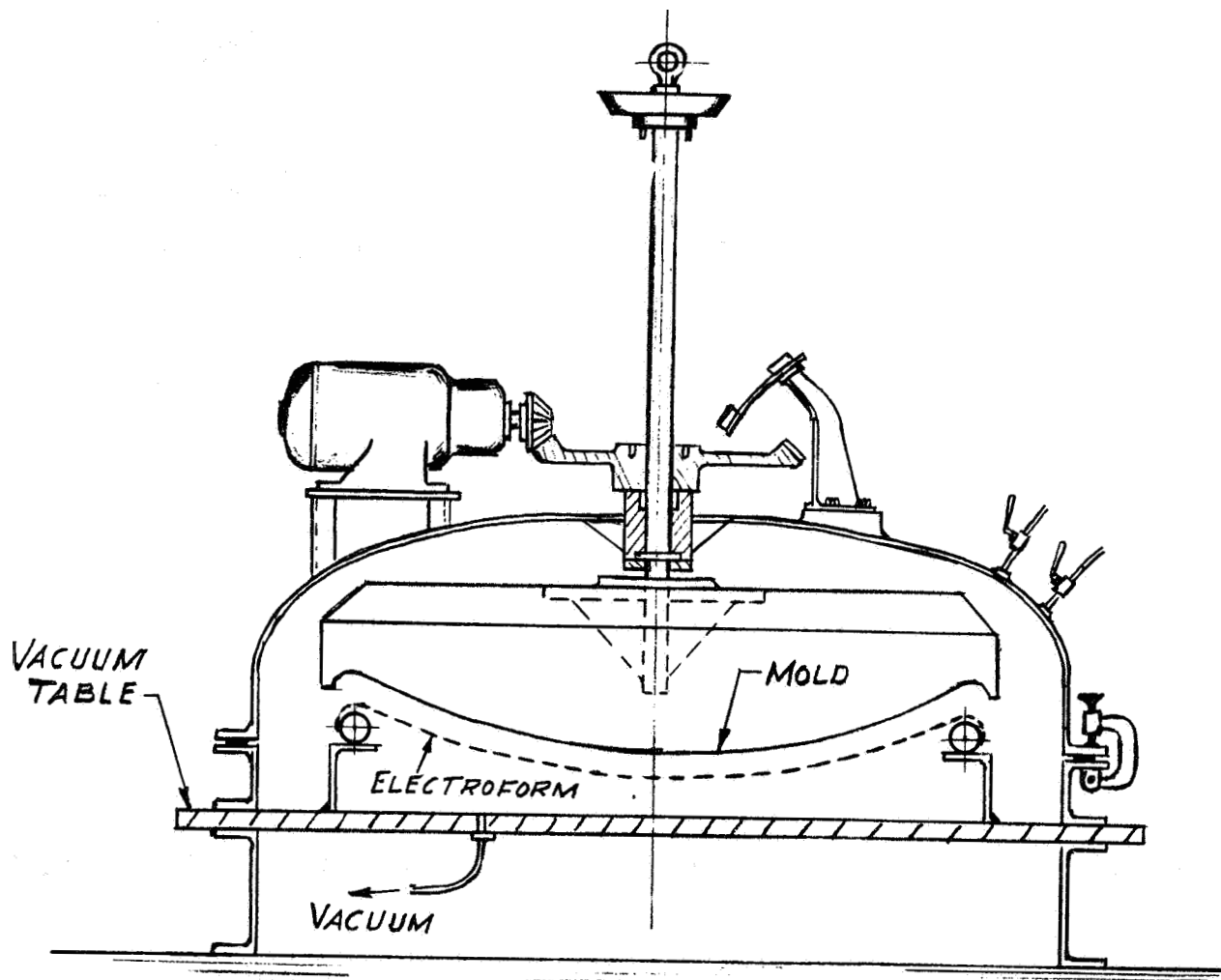
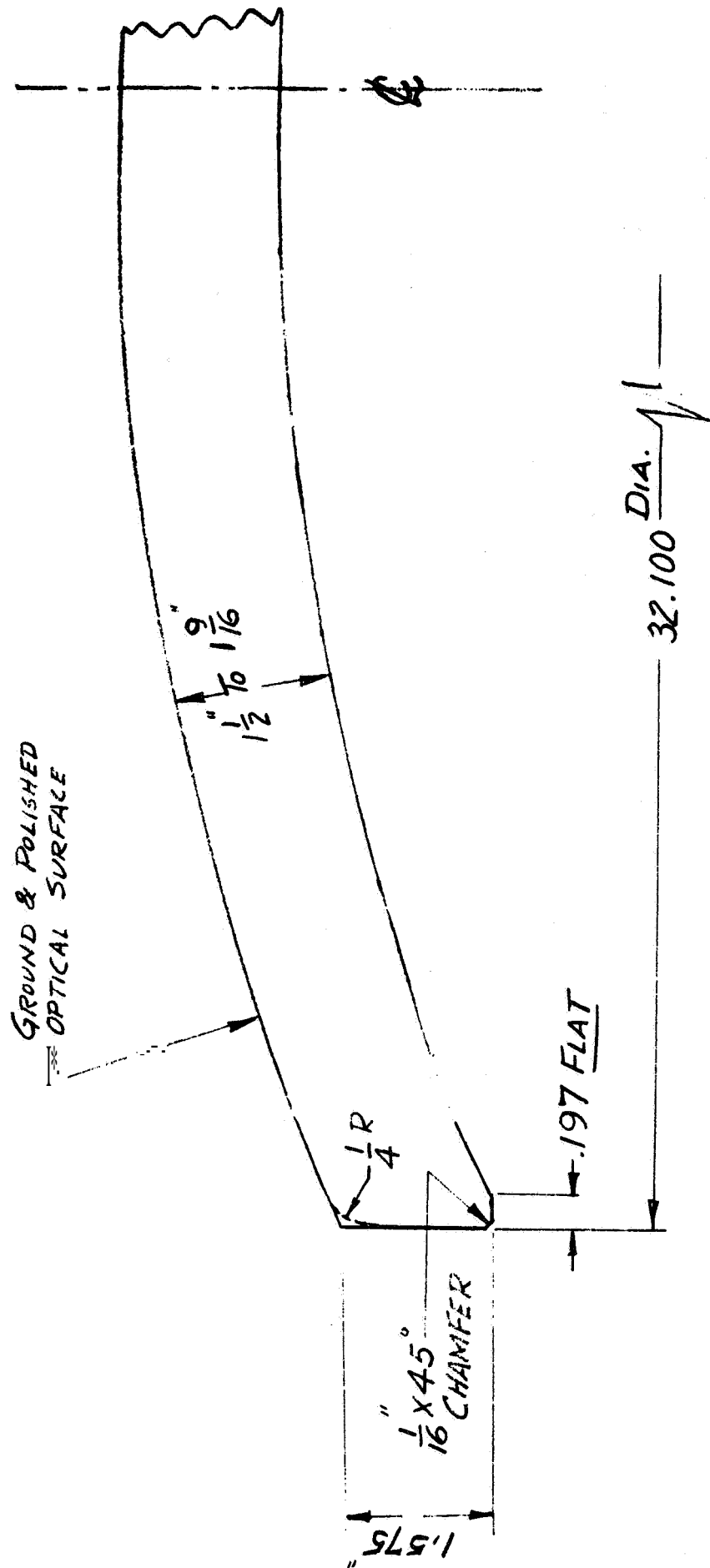


FIGURE 23      PARABOLIC GLASS MOLD  
 AS FABRICATED BY  
 FARRAND OPTICAL CO



FOCAL LENGTH -  $16.8''$   
 RIM ANGLE -  $48^\circ$



## APPENDIX A

### PHYSICAL PROPERTY MEASUREMENTS

#### Stress-Strain Curves

Tensile specimens, with a reduced cross-section of 0.220 inch x the given electroformed aluminum sample thickness, were machined.

Stress-strain curves were obtained from tests conducted on a Floor Model TT Instron Testing Machine, using an F-Cell for load pick-up. The cell was adjusted to 250 pounds full chart reading. Strain was measured using two strain gauges bonded to either face of the specimen by Eastman 910 adhesive. The strain gauge was attached over a one-inch length of the reduced area section. Stress-strain curves for several pertinent samples were obtained. Values of ultimate tensile strength, yield strength and per cent elongation were reported in another section.

#### Thermal Expansion

Test specimens, one half-inch wide, were machined and two lines were scribed spaced three inches apart.

Measurements were made by the method developed on Contract NAS 1-3309 (REF. 1). A Model KE-2 Keuffel and Esser Theodolite was mounted at a known distance from the specimen to measure the angle subtended by the 3-inch gauge length of the electroformed aluminum specimen. The change in gauge length was calculated from the measured change in the subtended angle which resulted from the temperature variation.

The test specimens were taped to an aluminum block to prevent buckling. The adhesive side of the tape was covered so that it did not exert any restraint on the specimen.

The specimens were placed in a Delta Design environmental chamber and sighted during test through a viewing port. The temperature range of  $-70^{\circ}\text{F}$  to  $+200^{\circ}\text{F}$  was selected. Measurements were made thirty (30) minutes after the specimen temperature had stabilized for each temperature cited above. A shielded thermocouple mounted on the gauge length surface of the specimen monitored the temperature during these measurements.

An average value of  $3.2 \times 10^{-6} / ^{\circ}\text{F}$  over the  $-70^{\circ}$  to  $+200^{\circ}\text{F}$  temperature range was measured for linear coefficient of thermal expansion of hollow silica microsphere-incorporated electroformed aluminum. An average value of  $11.8 \times 10^{-6} / ^{\circ}\text{F}$  was measured for an electroformed aluminum specimen lightly loaded with glass fibers. A value of  $10.5 \times 10^{-6}$  for a plain electroformed aluminum standard agrees with data from the previous contract.

## Density

The density of co-deposition electroformed aluminum composites was determined by the standard ASTM method. This specifies specimen volume determination by measuring the water displacement weight of the sample.

Density measurements of glass fiber-incorporated aluminum provided no meaningful data since the specific gravity of the two materials are almost identical. A density of 2.614 g/cc for hollow silica microsphere-incorporated electroformed aluminum was measured. This corresponds to a loading of 2.73 per cent by weight of the 0.26 g/cc microspheres. The density of these composites varies considerably with the loading fraction.

## Specular Reflectivity

Flat electroformed aluminum plates were electroformed over a glass plate. The specular reflectivity of a 2-inch x 3-inch specimen, incorporated with hollow silica microspheres, was measured at 100°F over the spectrum of 0.3 to 7.0 microns. A Beckman Model DK1L Reflectometer was used in the 0.3 to 2.7 micron range. For the 2.0 to 7.0 micron spectral range, the optical test specimen was measured in a Perkin-Elmer Model 205 Reflectometer. The tested specimen surface was "as removed" from the glass substrate - unpolished and uncoated. These data are reported in Table A1. Comparison is made with a comparable specimen which was vacuum coated with aluminum and with silicon monoxide. Values reported are absolute specular reflectivity based on a "standard" glass mirror, vacuum coated with aluminum.

## APPENDIX B

### ALUMINUM ELECTROFORMING PROCEDURE IN PILOT CELL

#### Preparation of the Glass Mold

1. Chemically clean and dry the glass mold.
2. Colloidal silver the outer edge and approximately 1" underneath mold,
3. Chemically clean the mold for silver spray coating.
4. Sensitize the silver spray mold including edges and under outside edge.  
(After mold is free of water breaks.)
5. Place mold into silver flash rack (Insert aluminum foil at contacts)  
and secure in place.

Note: Keep silvered mold wet with distilled water.

### Silver Plating of Glass Mold over Sprayed Silver

1. Attach the precontact wire to the flash rack, shown in Figure A1.
2. Lower mold into silver plating tank onto cathode bar.  
Note: Have current on (2-5 amps) as mold enters solution. Increase current to 25 amps five minutes after mold is fully submerged.
3. Silver plate (with agitation) at 6 asf (45 amps) for about one (1) hour.
4. Remove mold from bath, water rinse and dry.
5. Remove mold from silver flash rack.

### Aluminum Electroforming over plated Mold

1. Assemble the mold into aluminum plating rack (including cove assembly).
2. Place assembled rack onto "rack stand".
3. Attach wiper blade and adjust clearance.
4. Place the plating glove box on the "rack stand" over the plating rack, as shown in Figure A2.
5. Connect the precontact wire to the plating rack.
6. Hoist the plating rack assembly into the glove box.
7. Replace the glove box and contents back on the aluminum plating tank (connect gas lines and clamp down glove box). Note Figure A3.
8. Connect outside precontact wire to the cathode terminal.
9. Apply pretreatment solution to face of mold and cove ring.
10. Remove inside tank cover and place on the side wall of glove box.
11. Lower the plating rack assembly into the aluminum bath onto the D.C. contacts without stopping. See Figure A4.
12. Current to be applied to plating rack immediately after D.C. contact is made. Note: Electroforming area = 6 sq. feet (at 20 asf - 120 amps).
13. Connect gas lines to gas-driven motor on rack.
14. Adjust speed of mold rotation as required.
15. Start solution circulation:
  - a. Recirculation through filter and/or
  - b. Recirculation " by passing filter,
  - c. Adjustment of flow volume, as required,
  - d. Adjustment of current, as required.
16. Continue nitrogen purging of plating cell throughout the plating cycle. (Maintain 2-3 psi pressure).
17. Begin water cooling of the plating bath, adjusted as required.
18. Check recording instruments. (Should start-up prior to deposition).
19. Maintain constant checking and recording of data throughout the plating cycle.

#### Removal of Plating Rack Assembly from the Plating Unit at End of Cycle

1. Shut down plating current.
2. Shut off gas to rack motor and disconnect lines.
3. Raise plating rack assembly into glove box area. Allow mold to drain off entrained solution.
4. Cover plating tank. Clamp cover securely.  
Note: Continue necessary purging of tank and glove box.
5. Unclamp glove box, disconnect gas lines and outside precontact wire from plating tank.
6. Remove glove box and rack assembly from plating unit. Place on "rack stand", as shown in Figure A5.
7. Lower rack assembly onto rack stand. Disconnect inside precontact wire.
8. Replace glove box on plating cell and clamp in place. Connect gas lines.  
Note: Continue purging of plating cell.
9. Wash down plating rack assembly and electroformed aluminum with tap water.
10. Place plating rack assembly on loading table. Remove hold-down ring cove. See Figures A6 and A7.

#### Attachment of Torus to Cove of Electroformed Concentrator

1. Set torus in place. Position using spacers.
2. Inject epoxy between the torus ring and the cove, as seen in Figure A8. Allow epoxy to cure.
3. Trim epoxy overflow and remove spacers.
4. Clean for appearance.
5. Remove mold ring clamp (two halves).

#### Separation of Aluminum Electroformed Concentrator from Glass Mold

1. Remove flashing from the outer edge of the mold and bend upward away from mold surface.
2. Use nitrogen pressure under flashing to lift or start separation. Then lift up by torus ring very gently to separate electroform from mold.
3. If any liquid is evident on electroformed surface, quickly rinse with distilled water and dry.
4. Carefully remove flash from concentrator edge with sharp knife.

#### Reconditioning of Equipment for Repeated Cycle

1. Disassemble rack and mold. Water wash and dry.
2. Place glass mold in safe storage.
3. Clean all rack equipment and store away for next cycle.
4. Clean chemical silver spray equipment.
5. Clean D.C. contacts in aluminum plating cell.
6. Check and clean connections for gas-driven motor.
7. Check solution and make necessary additions.

## APPENDIX C

### OPTICAL INSPECTION OF MIRROR

#### Inspection Procedure

The mirror was mounted on a rotary table to facilitate multipoint inspection. The mirror was leveled and centered on the axis of rotation of the table. A beam on which a plunging-type theodolite was mounted, was positioned horizontally over the mirror. The focal point was found by locating a point source of light such that the image could still be observed in the theodolite as the mirror was rotated. The light source was adjusted to obtain the "best fit" condition.

The inspection was accomplished by leveling the theodolite successively over four radial positions and aligning the telescope to bring the lamp image to the center of the reticle. The angle of inclination from the vertical and the azimuth were recorded. The table was rotated to inspect each of 72 angular positions.

#### Optical Data

An existing computer program utilized for calculating the average slope error of the 9½-foot electroformed nickel mirror on Contract No. NAS 1-4105, was described previously (See Ref. 3). The collected data was reduced and is presented in Tables A2, A3 and A4 and Figures A9 thru A16, as produced by the computer recorder and the 7094 computer.

There were eight (8) points where the reading fell outside the field-of-view of the theodolite. This was caused by the lifting of the initial silver flash at the mirror edge. A very conservative value was recorded for these points, which reflects more the mirror condition than the probable "true" geometry. Note - 24 minutes of slope error was assumed. The average adjusted mean slope error was found to be 5.891 arc minutes. The median slope error was 4.674 arc minutes. The lifting of the flash at the periphery of the mirror should be considered in evaluating the geometry.

The adjusted slope error still was less than for any previously electroformed aluminum concentrator. The average slope error for two inspected mirrors on Contract NAS 1-3309 was 6.9 and 9.4 arc minutes, respectively.

Only one of the four mirrors produced under this contract was tested because of time limitations. By visual comparison, all four mirrors appeared equivalent.



1  
3  
3  
8  
7  
7  
3  
3  
3  
3  
3  
3  
8  
8  
9

# T A B L E   A   1

## SPECULAR REFLECTIVITY OF ELECTROFORMED ALUMINUM

<u>Wave Length, Microns</u>	<u>Specular Reflectivity</u> (As deposited, unpolished)	
	<u>Uncoated</u> <sup>c)</sup>	<u>Vacuum Coated with Aluminum and with Silicon Monoxide</u> <sup>d)</sup>
0.3 <sup>a)</sup>	58.2	83.1
0.4	84.0	87.3
0.5	87.0	88.1
0.6	89.5	88.2
0.9	95.1	87.2
1.2	96.2	93.7
1.5	97.7	95.6
1.8	97.9	95.8
2.1	98.2	96.5
2.4	98.2	96.3
2.7	98.0	96.0
2b)	96.7	95.3
3	97.0	95.3
4	96.1	95.9
5	96.2	96.2
6	96.2	95.8
7	96.3	96.0

a) Reflectivity determined with Beckman-Model DK1L Reflectometer for spectral range of 0.3 to 2.7 microns.

b) Reflectivity determined with Perkin-Elmer Model 205 Reflectometer for spectral range of 2-7 microns.

c) Aluminum incorporated with hollow silica microspheres.

d) Reported previously on Contract No. NAS 1-3309.

TABLE A2  
SUMMARY OF OPTICAL DATA  
30 INCH ALUMINUM MIRROR NO. 2

TELESCOPE	ALL STD. DEVIATIONS $\pm$ BY .0025 ARCHIN/DIVISION				AVERAGE SLOPE ERROR
	AVERAGE X READING	STANDARD DEVIATION	AVERAGE Y READING	STANDARD DEVIATION	
1	59.75	1.113	49.80	1.083	1.311
2	41.84	2.911	49.22	2.404	3.030
3	40.38	4.104	50.19	3.701	4.758
4	49.57	9.314	50.10	8.848	11.099

TELESCOPES 1-4  
AVERAGE X READING 46.72  
STANDARD DEVIATION 5.250

AVERAGE Y READING 51.27  
STANDARD DEVIATION 4.612

X VS Y  
AVERAGE 90.00  
STANDARD DEVIATION 6.098

TABLE A3  
RAW MEASURED SLOPE ERROR

ANGULAR POSITION (DEGREES)	TELESCOPE 1	TELESCOPE 2	TELESCOPE 3	TELESCOPE 4
0	3.543	2.803	3.344	3.553
5	3.543	3.711	3.880	7.447
10	3.794	3.788	3.394	3.927
15	1.047	4.445	3.160	7.458
20	1.445	4.454	3.491	2.501
25	2.514	5.941	4.339	5.563
30	2.701	3.145	3.711	7.587
35	2.512	4.484	5.532	3.920
40	2.847	5.574	7.587	8.510
45	2.345	7.710	6.119	4.410
50	1.444	6.121	6.047	8.454
55	2.235	7.055	9.453	11.359
60	1.674	5.550	12.395	8.123
65	3.744	7.099	7.112	7.587
70	1.445	5.199	2.949	5.124
75	2.048	4.603	7.043	9.234
80	2.228	5.009	8.427	15.132
85	2.331	4.084	7.592	12.402
90	1.445	5.912	4.239	12.350
95	2.419	0.495	2.649	7.579
100	2.434	1.701	1.445	13.403
105	2.154	2.035	3.501	4.703
110	2.444	6.323	7.052	23.547
115	2.449	0.711	3.991	23.547
120	2.444	3.015	6.044	23.547
125	2.288	1.047	5.577	23.547
130	1.884	2.035	7.233	23.547
135	1.120	6.392	11.855	23.547
140	1.042	2.303	9.997	23.547
145	1.273	3.193	1.243	14.450
150	1.488	4.709	14.780	23.547
155	1.488	6.074	6.880	15.581
160	2.034	3.345	11.455	14.781
165	3.545	7.055	7.953	12.774
170	1.184	6.845	5.913	8.108
175	1.052	9.123	2.504	7.000
180	1.492	6.505	0.335	7.458
185	2.352	2.942	2.228	13.321
190	2.071	6.391	4.719	4.344
195	1.444	6.497	6.917	4.442
200	0.729	7.215	6.288	10.953
205	0.999	5.358	2.021	14.277
210	1.170	5.420	8.853	11.303
215	1.444	4.717	8.242	13.914
220	0.734	5.009	7.902	8.547
225	1.444	5.544	7.439	12.429
230	1.444	5.911	3.347	10.347
235	2.255	8.040	2.051	10.704
240	2.038	3.841	4.144	11.394
245	2.043	2.021	1.450	6.379
250	2.043	2.341	2.548	5.850
255	2.291	4.155	8.274	18.044
260	3.300	4.423	6.737	8.032
265	3.300	4.282	1.723	14.730
270	2.801	2.341	5.298	14.772
275	2.434	2.458	7.454	11.481
280	3.004	5.778	8.051	7.430
285	2.908	6.944	8.243	7.440
290	4.403	4.845	6.220	11.735

TABLE A3 (Concl'd)

295	3.720	0.387	1.352	11.918
300	3.850	4.299	3.528	10.351
305	5.100	1.255	3.528	4.218
310	4.751	3.299	4.942	5.037
315	4.755	2.549	6.052	9.399
320	4.918	3.675	6.160	8.144
325	5.195	5.190	3.376	8.599
330	4.918	0.878	6.987	7.499
335	5.384	1.748	9.943	8.199
340	5.062	2.234	8.975	14.337
345	4.936	3.832	9.968	9.812
350	0.998	0.947	4.728	9.099
355	4.810	0.840	1.619	9.812
MEAN	3.556	3.689	5.323	10.998
STD.DEV.	1.060	1.856	2.992	9.766
TELESCOPES 1-4 (ALL READINGS)				
MEAN SLOPE ERROR	5.891			
STD. DEVIATION	7.453			
MEDIAN SLOPE ERROR	4.674			

TABLE A4  
ADJUSTED SLOPE ERROR

ANGULAR POSITION (DEGREES)	TELESCOPE I	TELESCOPE 2	TELESCOPE I	TELESCOPE A
0	4.859	0.783	2.104	6.449
5	4.843	2.872	3.789	8.944
10	5.019	e.957	4.901	4.242
15	2.298	3.412	2.558	7.012
20	2.347	3.898	2.955	1.947
25	3.759	4.759	4.110	5.745
30	3.984	1.989	2.872	6.418
35	3.795	3.105	4.921	4.172
40	4.146	4.974	7.104	9.734
45	3.444	C.975	5.048	3.741
50	2.445	5.124	4.904	7.912
55	3.534	6.057	8.595	10.157
60	3.158	4.342	11.192	7.380
65	5.047	6.023	5.838	6.418
70	2.914	4.071	1.449	4.141
75	3.250	3.345	5.808	1.050
80	3.445	3.785	7.148	11.065
85	3.575	2.840	6.320	11.475
90	2.914	4.494	5.084	12.499
95	3.491	1.850	2.449	8.357
100	3.848	2.512	1.702	14.105
105	3.371	3.282	2.514	5.850
110	3.941	7.593	7.251	24.101
115	3.770	0.459	7.289	24.101
120	3.941	3.135	7.327	24.101
125	3.583	2.103	6.536	24.101
130	3.185	7.784	8.186	24.101
135	2.404	7.320	12.955	24.101
140	t.323	3.541	11.099	24.101
145	t.554	1.980	2.522	17.164
150	2.770	4.351	14.530	24.101
155	7.770	5.803	5.408	14.799
160	3.106	t.454	10.489	18.073
165	4.423	6.057	6.813	11.501
170	2.052	5.652	4.652	6.850
175	1.824	8.602	1.245	s.195
180	7.633	5.487	1.627	7.378
185	3.347	1.658	2.029	13.121
190	3.323	5.092	1.420	5.599
195	7.665	5.227	5.645	5.275
200	1.887	6.020	4.957	10.407
205	2.242	4.067	0.723	13.003
210	2.325	4.398	7.570	10.019
215	1.950	3.405	6.983	12.842
220	1.496	3.783	6.787	8.146
225	2.445	4.296	6.941	12.348
230	2.445	4.410	3.140	10.747
235	3.085	7.173	2.747	11.838
240	3.035	2.441	3.195	12.618
245	2.945	0.723	2.951	7.669
250	2.945	1.973	1.915	6.966
255	3.253	2.858	7.350	17.801
260	4.234	3.356	5.912	7.020
265	4.234	3.011	0.451	13.867
270	1.923	1.973	4.492	13.821
275	3.803	1.471	6.335	10.180
280	4.234	5.848	6.758	7.595
285	4.203	1.744	6.962	8.258
290	9.388	2.818	4.945	12.489

TABLE A4 (Concl'd)

29F	2.649	1.985	2.649	10.740
300	4.811	4.413	4.048	9.217
30F	3.899	2.718	4.048	3.018
310	3.915	2.949	6.019	9.749
319	3.498	3.919	7.091	9.949
320	3.649	4.543	7.081	9.073
32H	3.912	4.985	4.043	9.433
330	3.649	1.095	7.903	8.419
339	4.100	3.705	9.398	9.398
340	3.877	3.498	10.276	15.738
345	3.700	4.985	11.145	10.988
350	0.333	2.035	6.024	9.237
355	3.528	0.518	2.887	10.100
YAY	2.394	4.374	5.948	11.095
STD.DEV.	1.008	1.957	2.950	5.648
TELESCOPES 1-4 (ALL READINGS)				
MEAN SLOPE ERROR	5.953			
STD. DEVIATION	4.636			
MEDIAN SLOPE ERROR	4.643			

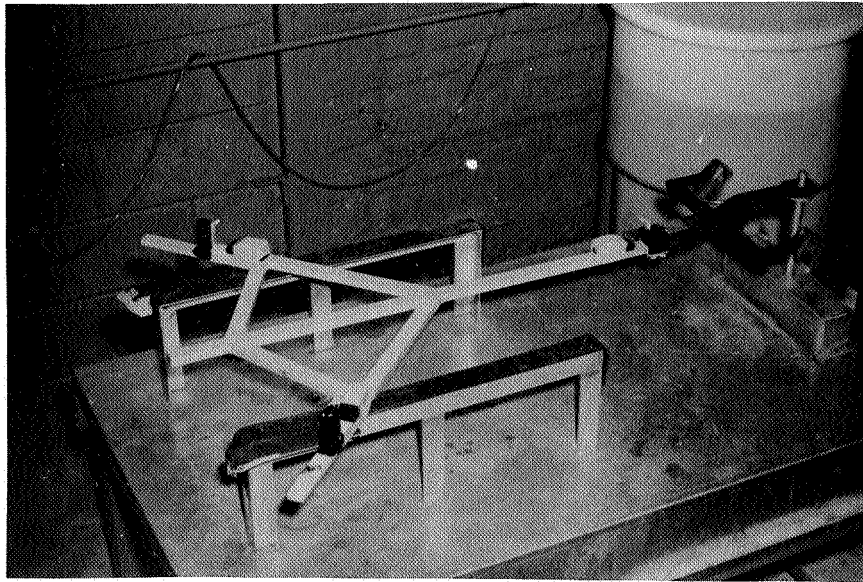


Figure A1. Flash rack for 30-inch diameter glass mold.

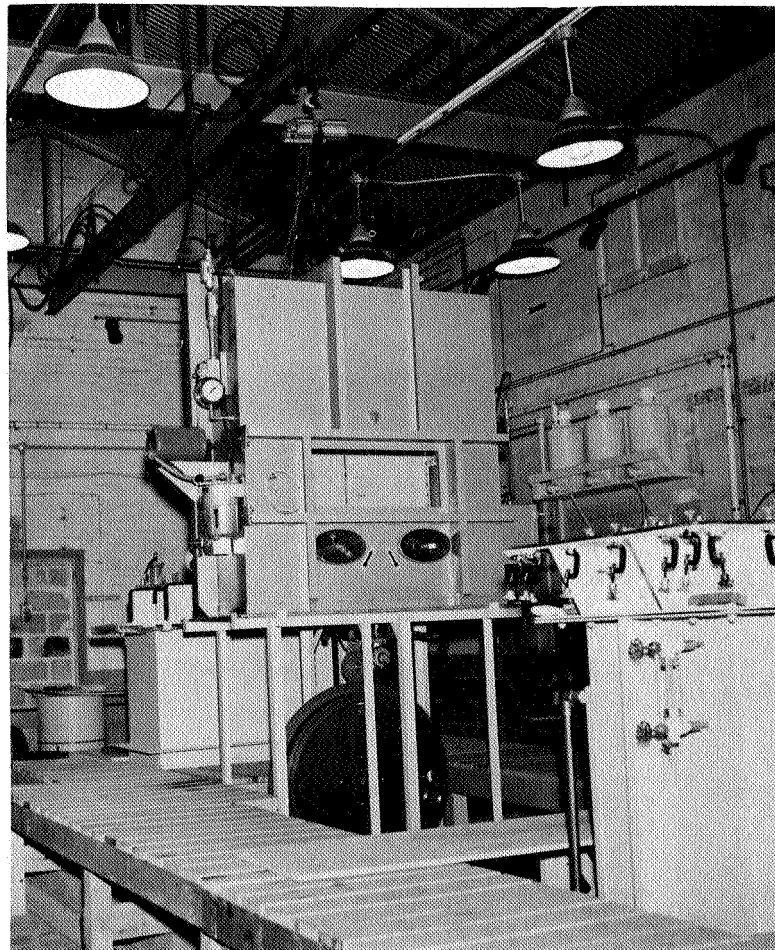


Figure A2. Placement of plating tank glove box enclosure on mock-up stand over plating rack. Note shelf on right wall supporting silvering solutions, demineralized water for applying conductive film on glass mold.



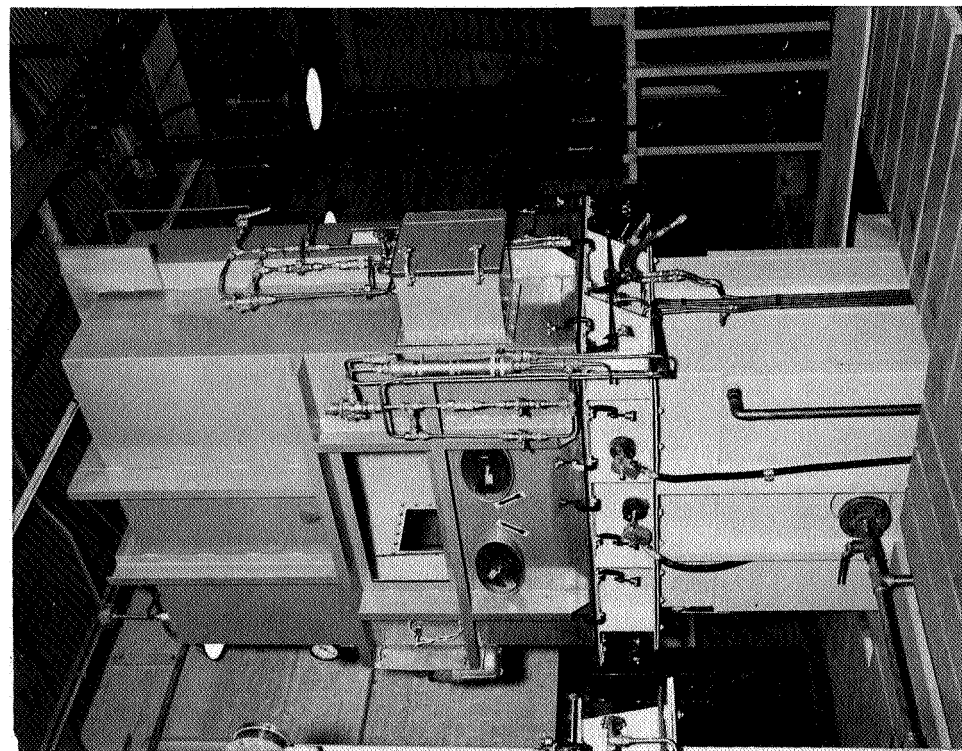


Figure A3. Front view of plating tank and glove box enclosure. Note gloves were removed to expose bung hole cover which permits pressurizing interior.

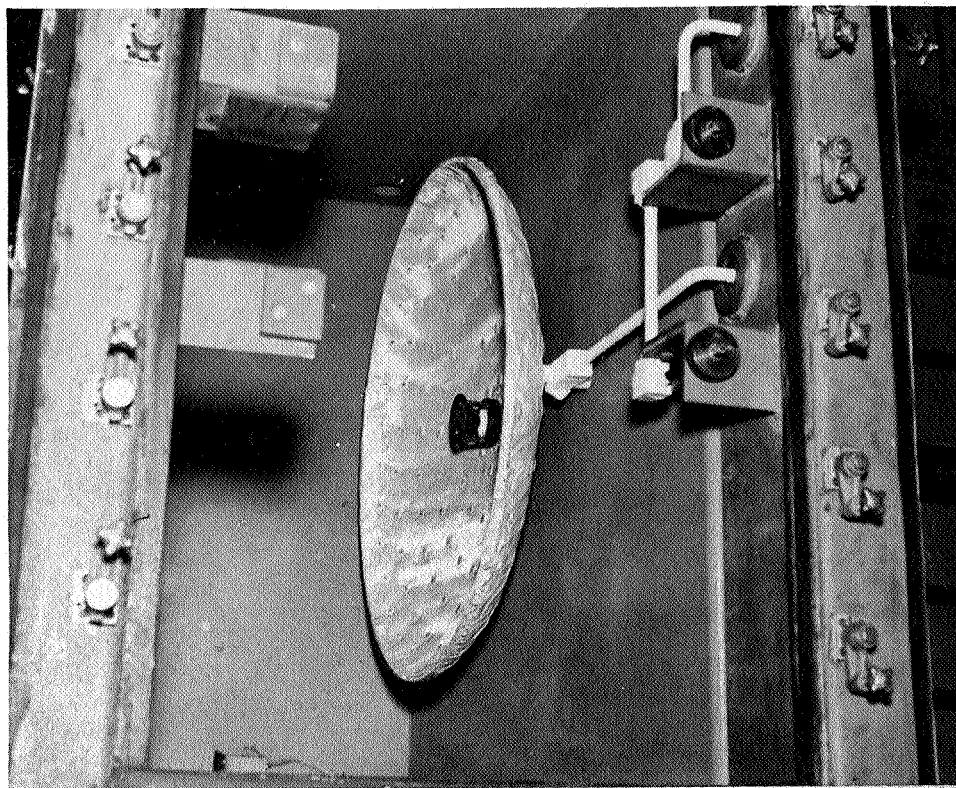


Figure A4. Interior view of plating tank (glove box removed). Note the anode bagging and inner baffle for desired dispersion of fiber-containing solution. Upper brackets position and provide electrical connection to rack containing mold.

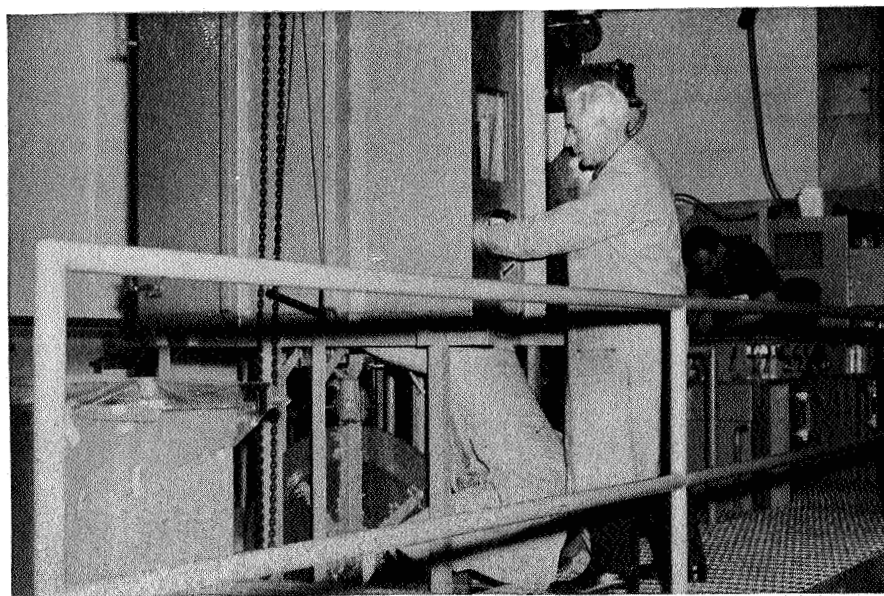


Figure A5. Lowering glass mold rack from plating tank glove box enclosure. Note growth of "trees" on backside of plating rack through TFE insulation.

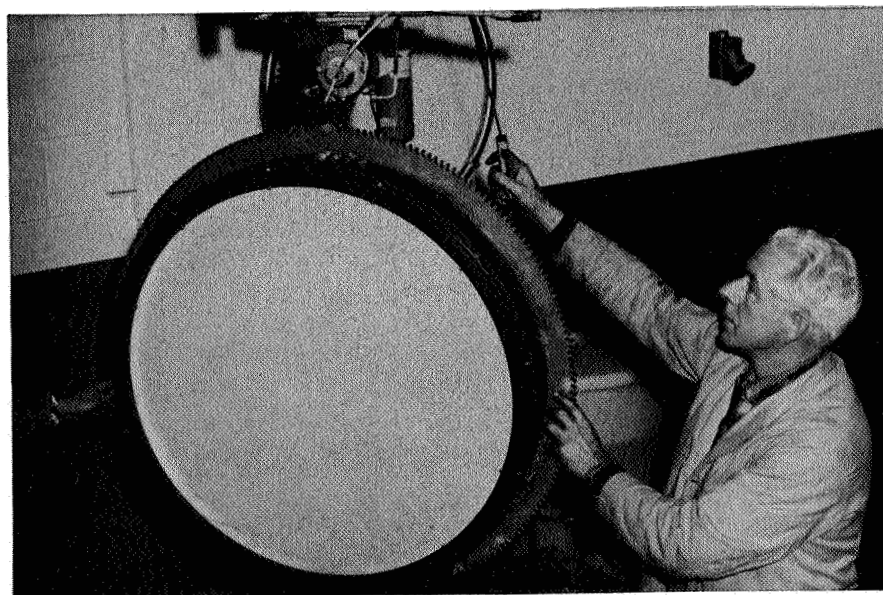


Figure A6. Transporting the plating rack and aluminum electroform to loading table.



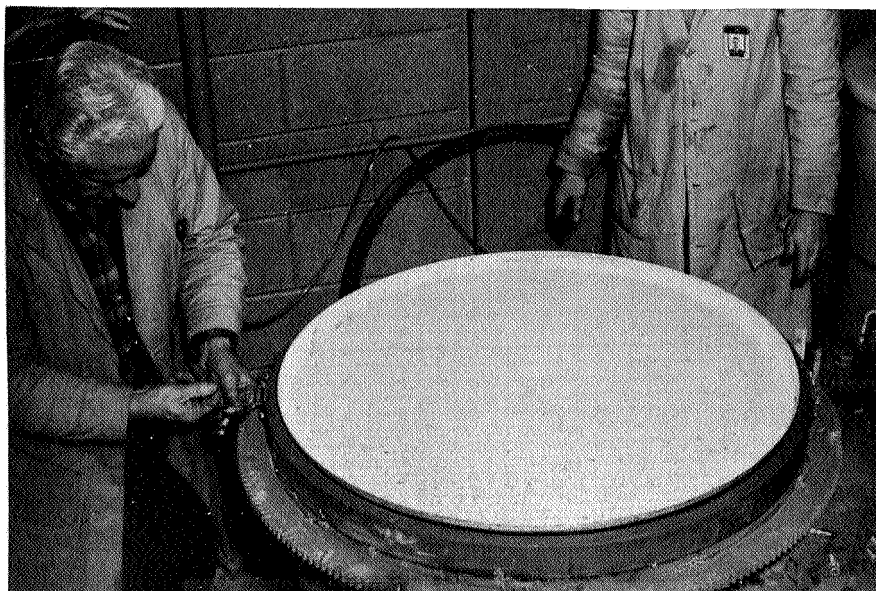


Figure A7. Hold down ring for cove removed in preparation for bonding torus ring to electroform for structural support.

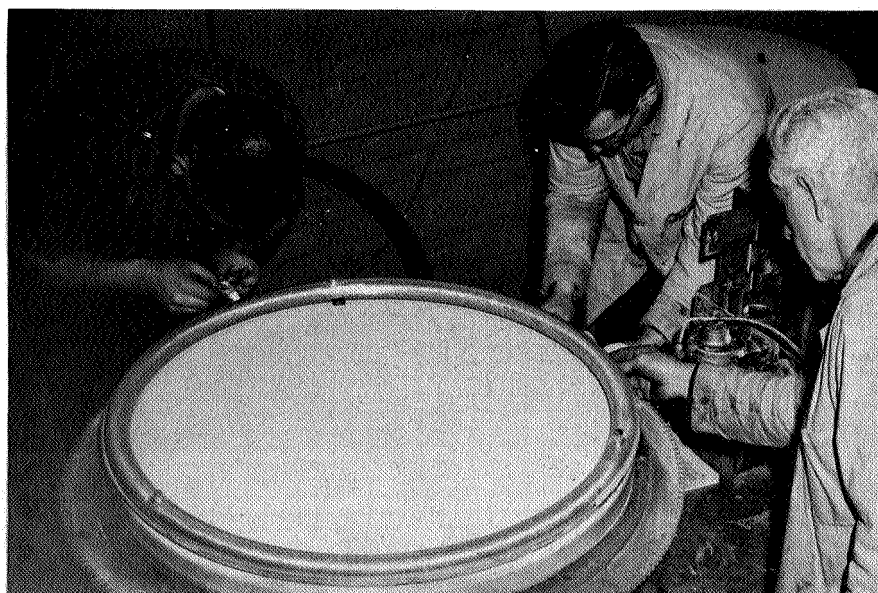


Figure A8. Epoxy being injected to bond torus ring to cove of electroform. Note the spacer under boss in torus.

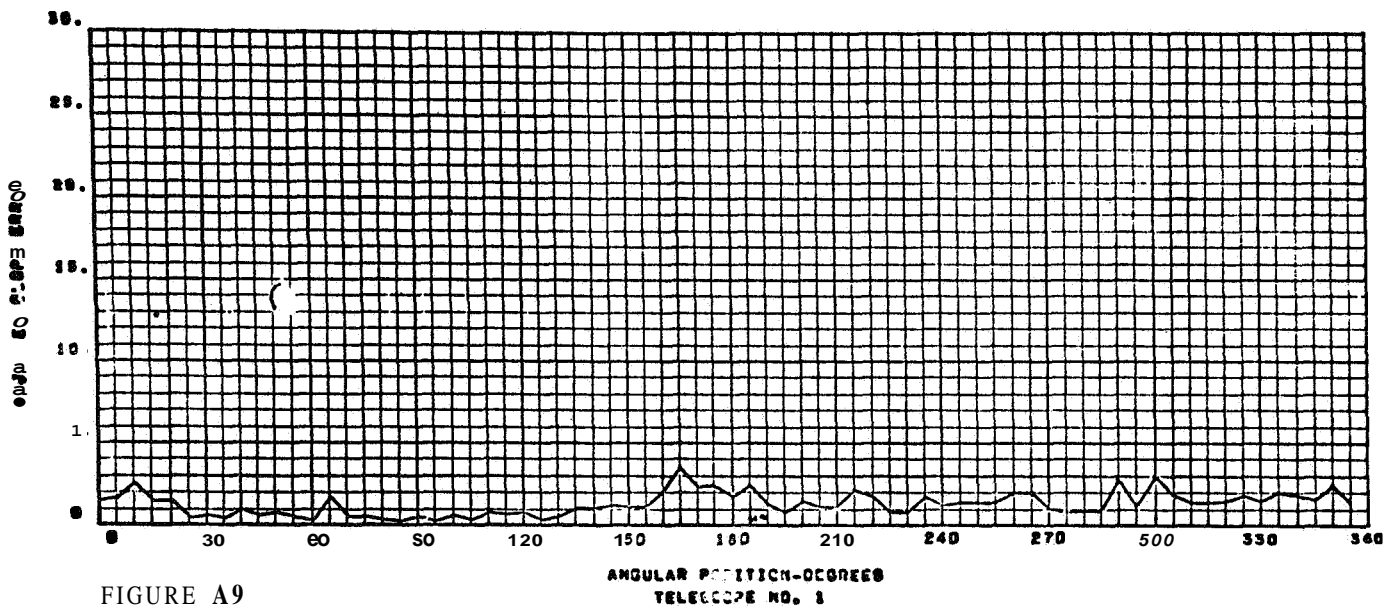


FIGURE A9

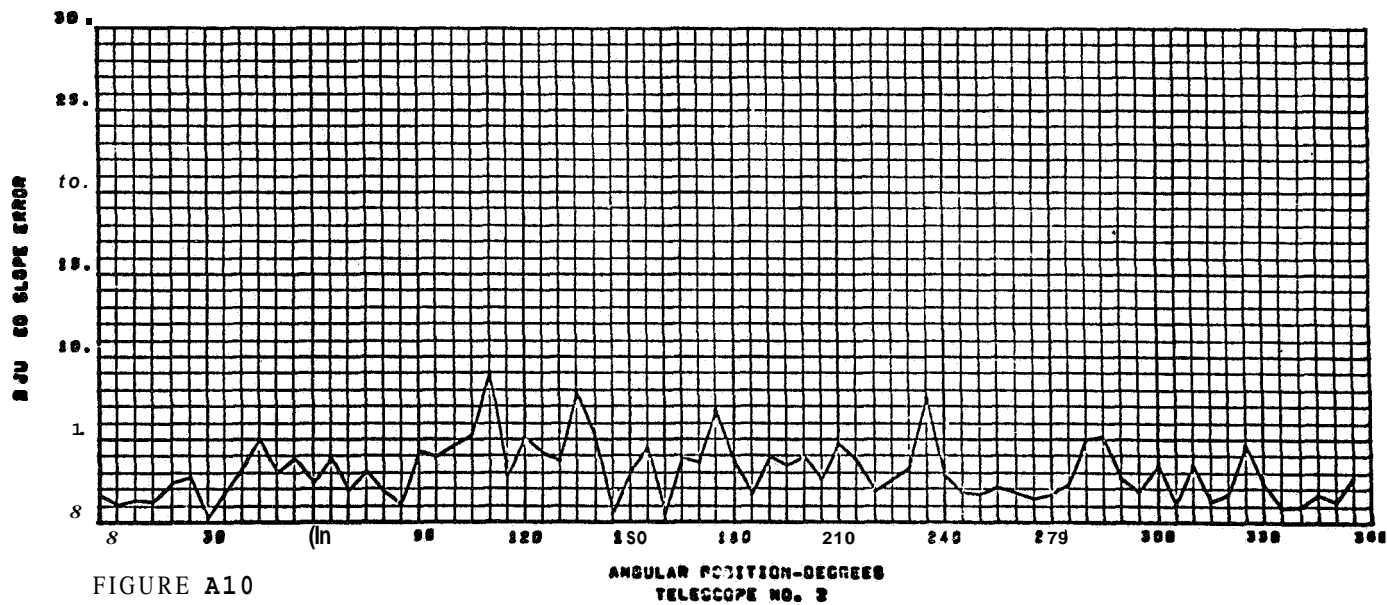


FIGURE A10

$$\text{ADJUSTED SLOPE ERROR} = \sqrt{(X_N - \bar{X}_N)^2 + (Y_N - \bar{Y}_N)^2}$$

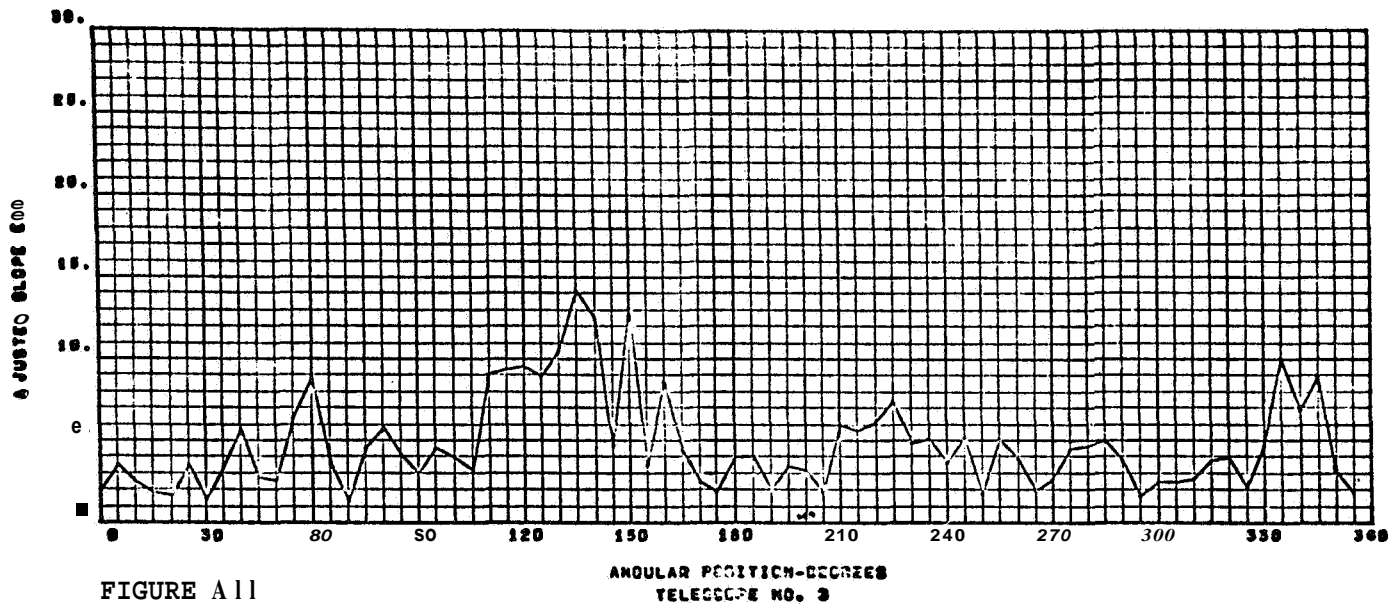


FIGURE A11

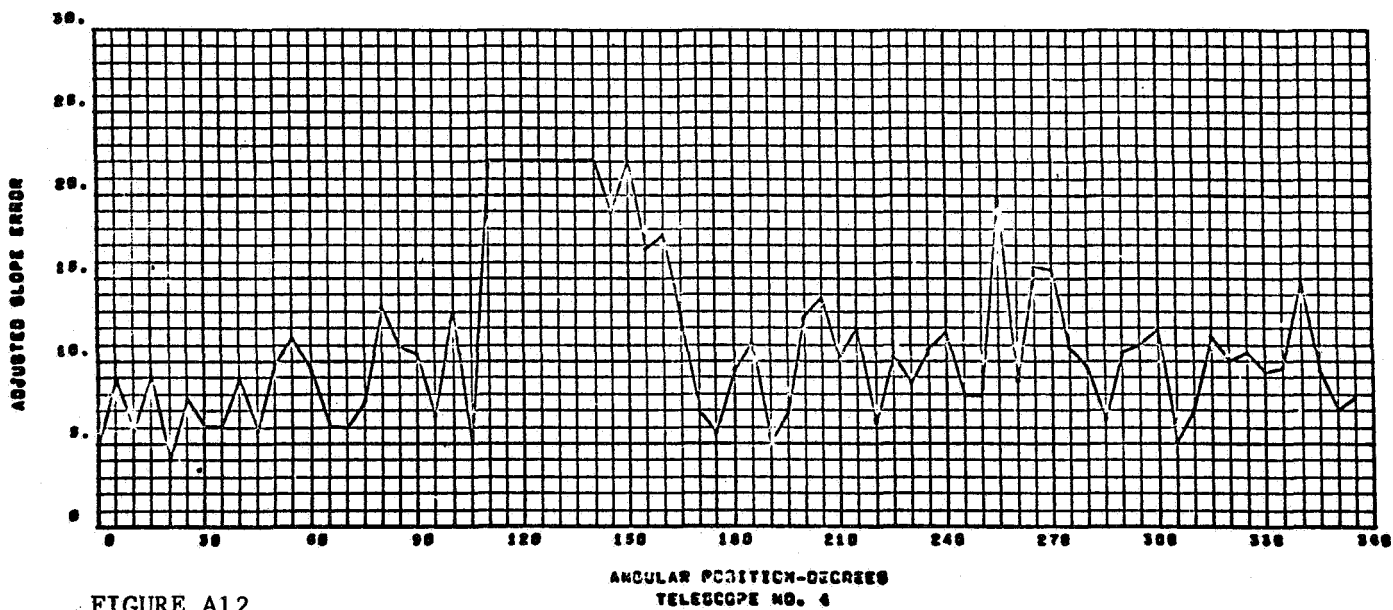
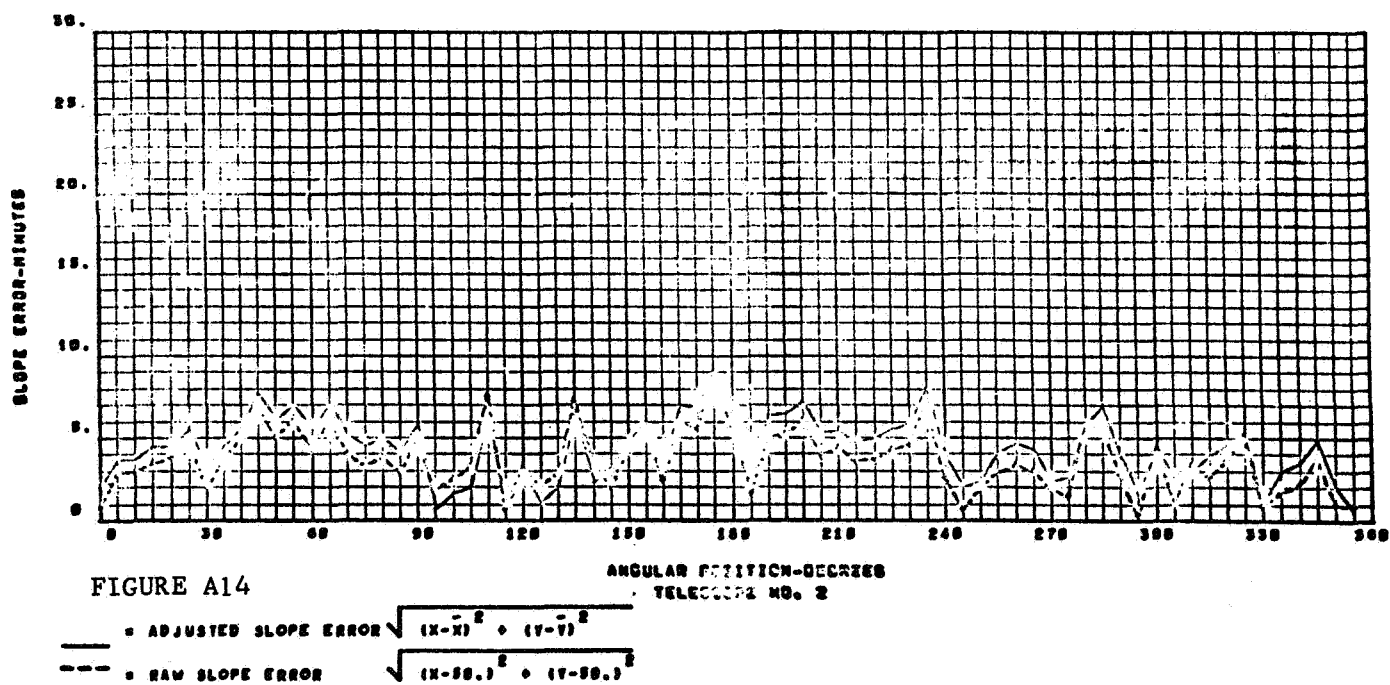
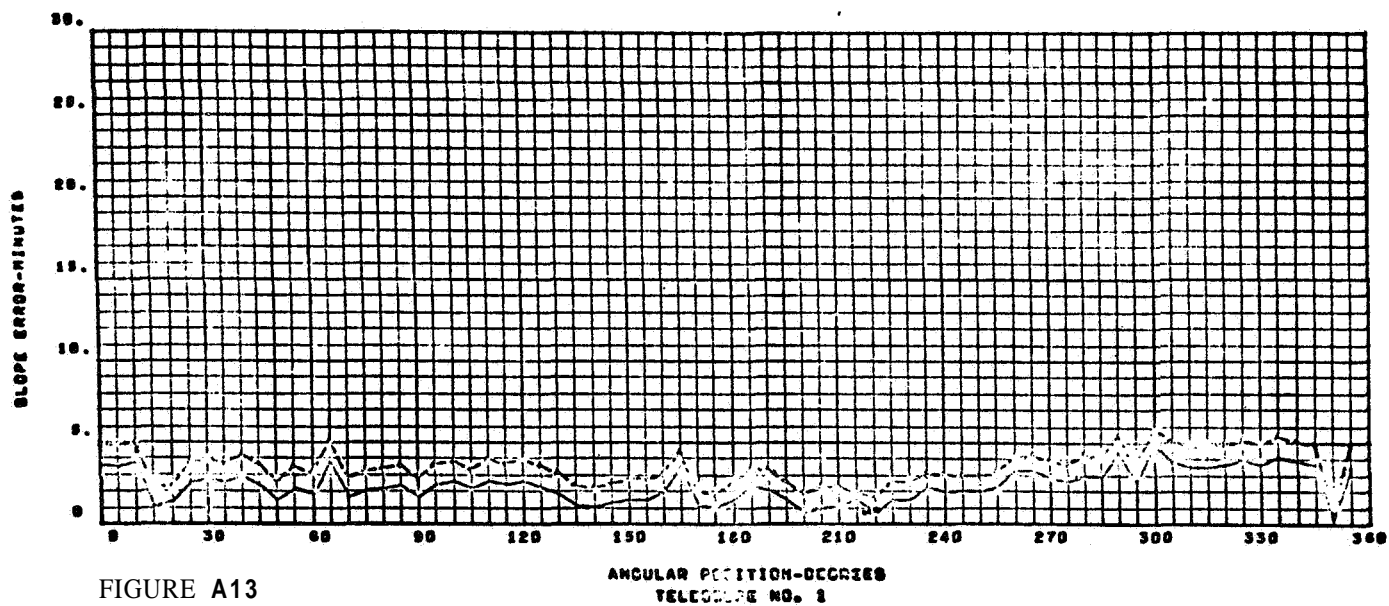
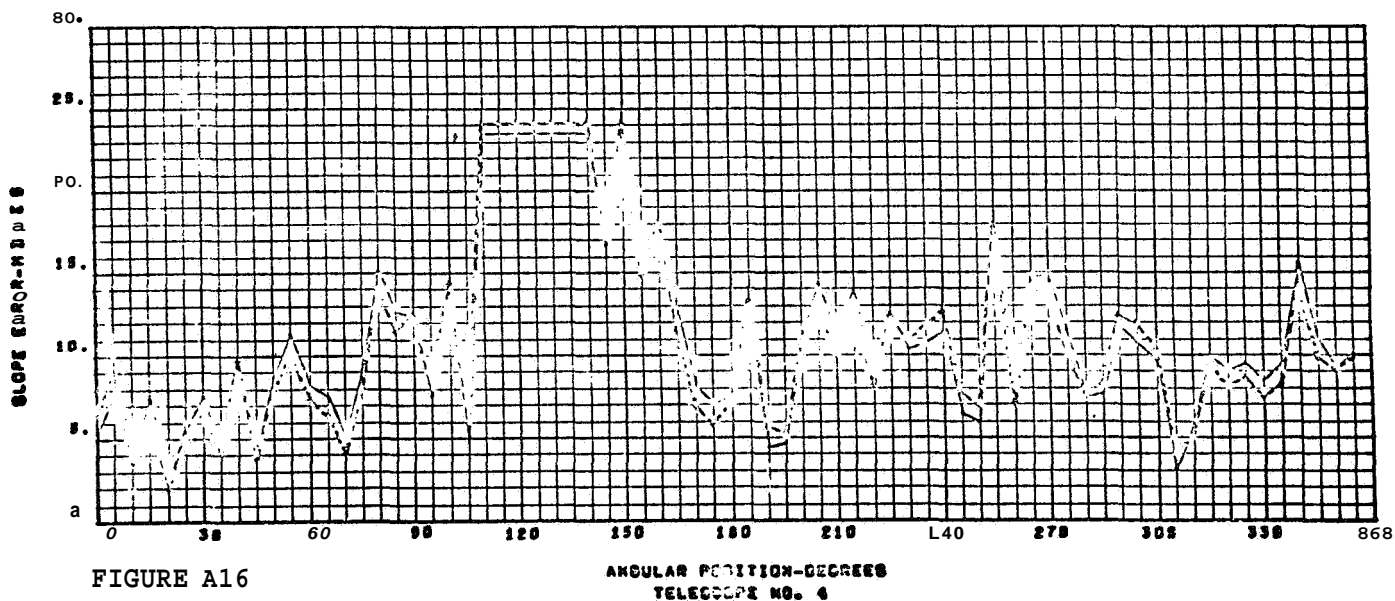
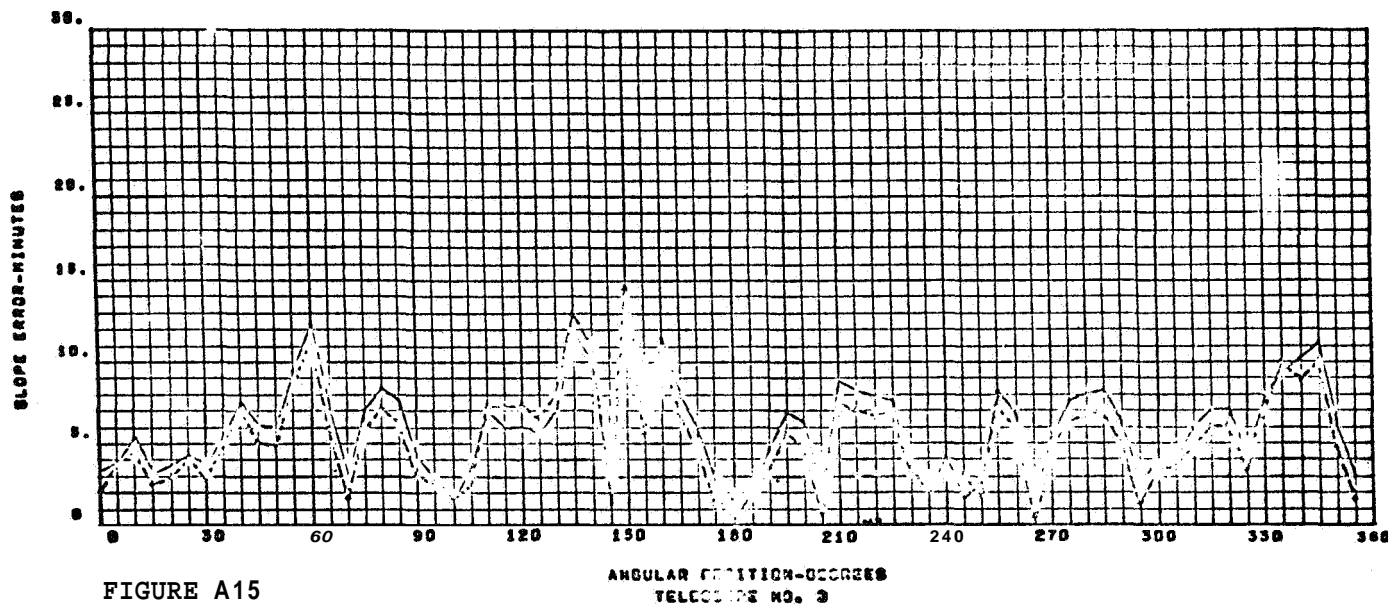


FIGURE A12

$$\text{ADJUSTED SLOPE ERROR} = \sqrt{(X_N - \bar{X}_N)^2 + (Y_N - \bar{Y}_N)^2}$$



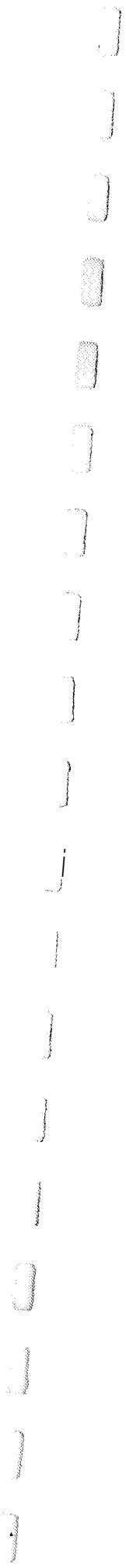




— = ADJUSTED SLOPE ERROR  $\sqrt{(X-\bar{X})^2 + (Y-\bar{Y})^2}$   
 --- = RAW SLOPE ERROR  $\sqrt{(X-\bar{X}_R)^2 + (Y-\bar{Y}_R)^2}$



1/6/67



#### REFERENCES

1. Schmidt, Ferenc J.; and Hess, Irving J.: Electroforming Aluminum for Solar Energy Concentrators. NASA CR-197, 1964.
2. Conner, J. H., and Brenner, A.: Electrodeposition of Metals from Organic Solutions. J. Electrochem. Soc., 103, p. 657-662 (1956).
3. Anon.: 9.5-Foot Paraboloidal Master and Concentrator. NASA CR-66122, 1966.